ORIGINAL PAPER

Implementation of a non-destructive method to assess weathering deterioration of sandstones in cultural heritage

Elisa Mammoliti[1,2] · Marta Cupido[3] · Riccardo Teloni[4] · Francesca Tittarelli[2] · Gabriele Giuli[1] · Eleonora Paris[1] · Piero Farabollini[1] · Stefano Santini[3]

Abstract

This paper proposes a non-destructive approach based on the Equotip hardness tester to assess weathering deterioration in a protected sandstone monument located in the historic centre of Camerino (Italy). The approach is tested on one sandstone column, where various forms of weathering, such as discolouration, scaling and loss of stone volume, are observed. The mechanical characterisation with Equotip was performed on 24 measuring points, systematically distributed in the column. Innovatively, the two probes available from Proceq (Proceq© 2010) were used to assess differences among surface and in-depth hardness values of the column. In addition, an un-weathered rock core from the original extraction site was also analysed and compared with the rock matrix of the column. The obtained results show a 15% hardness reduction from depth to the surface of the column and a 25% overall hardness reduction with respect to the fresh sandstone core samples. Equotip results were coupled with grain size analyses, mercury intrusion porosimetry, scanning electron microscopy and X-ray diffractometry results, and a correlation between hardness and grain size was evaluated. By combining these approaches, it was possible to identify the processes that occurred during weathering: (a) freeze-thaw cycles that caused a decrease in micropore volume and an increase in macropores connected with low Equotip values; (b) iron oxide and sulphuric acid released from pyrite oxidation contribute to the dissolution and precipitation of calcium carbonate, which can be rearranged in the outer and surface macroporosity. The quantitative approach proposed in this study may be a valid low-cost and quick tool to assess weathering heterogeneities on building stone materials and to provide insights for effective preservation strategies of historical monuments.

Keywords Building stone · Sandstone · Weathering · Equotip hardness tester · Deterioration assessment · Cultural heritage

Introduction

The deterioration of building stones is a particularly important problem in countries rich in cultural heritage such as Italy, which has the highest number of UNESCO World Heritage Sites (MIC — Ministero della Cultura 2023). To reach sustainable monument preservation and to program restoration interventions, detailed information regarding stone mineralogy, texture, porosity etc. is an essential parameter to be assessed. However, one of the complexities in the characterisation of stone materials is the variation in mechanical properties and alteration as a function of rock heterogeneity. This is more pronounced in sedimentary and metamorphic rocks, which are typically characterised by variability in grain size, mineralogy and macro-/microstructure, clearly influencing the mechanical properties and durability of the rock

✉ Marta Cupido
  m.cupido@campus.uniurb.it

1 Scuola di Scienze e Tecnologie, Sezione Geologia, Università degli Studi di Camerino, Via Gentile III da Varano 7, 62032 Camerino, MC, Italy

2 Dipartimento di Scienza e Ingegneria della Materia, dell'Ambiente e Urbanistica (SIMAU), Università Politecnica delle Marche (UNIVPM), Via Brecce Bianche, Ancona 60131, AN, Italy

3 Dipartimento di Scienze Pure e Applicate (DiSPeA), Università degli Studi di Urbino Carlo Bo, Via Ca' Le Suore 2, Urbino 61029, PU, Italy

4 GeoMORE s.r.l, Spinoff di Geologia, Università degli Studi di Camerino, Via Gentile III da Varano 7, 62032 Camerino, MC, Italy

(Kong et al. 2021). Since the weathering process will be influenced not only by external influences (climate, air pollution) but also by a stone's petrographic characteristics (Götze and Siedel 2004; Török and Přikryl 2010), accurate petrographic data are important to predict the expected weathering behaviour of a fresh sandstone. Especially in highly heterogeneous rocks such as sandstones (Siegesmund et al. 2002), surface alteration may occur in different forms and at different scales (Viles et al. 1997) and with different causes of damage (Turkington and Paradise 2005), such as (a) chemical processes related to the effects of atmospheric pollution and the development of crusts (Török 2003, 2008; Belfiore et al. 2013; Alexandrowicz et al. 2014; Marszałek et al. 2014); (b) physical decay in the form of salt crystallisation (McGreevy 1985; Bai et al. 2003) and phenomena associated with the increase in porosity of the stone (Jeannette 1997; Benavente et al. 2004; Adamovic et al. 2011; Molina et al. 2011; Liu et al. 2019, 2021; Jia et al. 2019; Huang et al. 2022); (c) hydric expansion due to the presence of clay minerals (Veniale et al. 2001; Jiménez-González et al. 2008; Sebastián et al. 2008); (d) colour change due to the alteration of ferrous minerals (Sebastián et al. 2008; Marszałek et al. 2014).

Although it is well known in the literature that mineralogical and physical properties of rocks influence their mechanical behaviour (Cantisani et al. 2013; Bozdağ et al. 2020; Salvatici et al. 2020; Wang and Zhang 2023), to our knowledge, there has been no study aimed at testing the use of Equotip hardness tester in correlation with mineralogical and physicochemical parameters of rocks. In fact, most of the authors correlate Schmidt hardness with the porosity system (Hatır et al. 2019; Chen et al. 2019; Salvatici et al. 2020; Le et al. 2022; Qi et al. 2022; Wang and Zhang 2023), with the capillary effect (Bozdağ et al. 2020), with the high or low content in $CaCO_3$ cement (Cantisani et al. 2013; Salvatici et al. 2020) or with surface moisture (Sumner and Nel 2002; Hatır et al. 2019; Kósa and Török 2020).

In the scientific literature, the Schmidt hammer is very popular in comparison to the Equotip, and it is used for a wide variety of studies such as weathering maps (İnce et al. 2018; Theodoridou and Török 2019; Bozdağ et al. 2020; Korkanç et al. 2021; and literature therein) and provenance studies (Aksoy et al. 2021). However, due to its high impact energy, its use is discouraged on soft, porous and/or easily damaged/weathered stones (Williams and Robinson 1983; Goudie 2006; Aydin 2014; Mammoliti et al. 2021; Přikryl and Snížek 2023). Thanks to its 66 times lower impact energy, the Equotip hardness tester is instead recommended for weathering studies in a wide range of rocks at different stages of weathering and strength (Aoki and Matsukura 2007; Viles et al. 2011; Mol and Viles 2012; Cutler et al.

2013; Coombes et al. 2013; Wang et al. 2020, 2021), as well as for detecting minor changes in surface hardness (Aoki and Matsukura 2007; Viles et al. 2011; Alberti et al. 2013; Wang et al. 2020; Tonon et al. 2022).

In contrast to destructive approaches such as uniaxial compressive strength test (UCS) (Basu et al. 2009; Witzany et al. 2010; Přikryl et al. 2011; Ludovico-Marques et al. 2012; Cantisani et al. 2013; Přikryl and Snížek 2023), penetration tests (Mohamad et al. 2008), creep tests (Verstrynge et al. 2014), flat-jack tests and diagonal compression tests (Lombillo et al. 2013; Andreini et al. 2014), rebound-based hardness testing such as Equotip does not require invasive material sampling. For this reason, the mechanical testing approach with Equotip is a valid tool for countries such as Italy where invasive sampling in historically protected buildings is not permitted without previous special permission from the Superintendence of Cultural Heritage. Surface hardness is only one of the non-destructive tests available for investigating mechanical building material properties, and it is increasingly adopted over other techniques (Vasanelli et al. 2013; Cutler et al. 2013; Fort et al. 2013; Zhang et al. 2019; Chen et al. 2019; Theodoridou and Török 2019; Bozdağ et al. 2020; Mammoliti et al. 2021; Wang et al. 2021). These include P-wave velocity (Popovics 2003; Siedel et al. 2010; Vasanelli et al. 2013; Fort et al. 2013; Christaras et al. 2016; Zhang et al. 2019; Chen et al. 2019; Bozdağ et al. 2020), surface moisture (Cutler et al. 2013; Theodoridou and Török 2019), infrared thermograph imaging (Popovics 2003; Schuller 2003; Olmi et al. 2016; Pappalardo et al. 2022) and drilling resistance (Pamplona et al. 2007; Siedel et al. 2010; Al-Naddaf et al. 2012; Manganelli Del et al. 2016; Chen et al. 2019).

The aim of this research is to implement a non-destructive method based on Equotip to evaluate the relationship between the hardness of rock surface and depth with building stone alteration derived by physicochemical and mineralogical analyses, including grain size and pore structure. The methodology was applied in the historic city centre of Camerino (Marche Region, Central Italy), which suffered significant damages due to the seismic sequence that struck Central Italy in 2016–2017 and where sandstone is a predominant construction material. One of the main innovations of this study concerns the combined use of the two probes available for Equotip model Piccolo 2 (Proceq© 2010) for in situ measurements: the D probe (surface probe) and the additional DL-type (in-depth probe).

Thanks to this approach, it was possible to deeply investigate sandstone alteration from a non-invasive mechanical point of view, overcoming the difficulties in characterising a historically protected rock material and then validating portable non-destructive technology for alteration studies.

Geology, construction and building stones

The town of Camerino (Marche Region, Central Italy) is located on the top of a hill, between the valleys of Chienti and Potenza rivers, and, from a geological standpoint, is part of the Camerino Turbiditic Basin, which extends from Albacina to Visso (Calamita et al. 1977). The turbidite deposits (Middle Tortonian–Messinian), specifically defined as Camerino Geological Formation (Fm.), lie on the hemipelagites of the Bisciaro-Schlier sequence, while on top, they are covered by the Gessoso-Solfifera Fm.

The work is focused on the small arcade of Palazzo Ducale, which is one of the main historical buildings of Camerino town (Fig. 1a). Palazzo Ducale is a complex
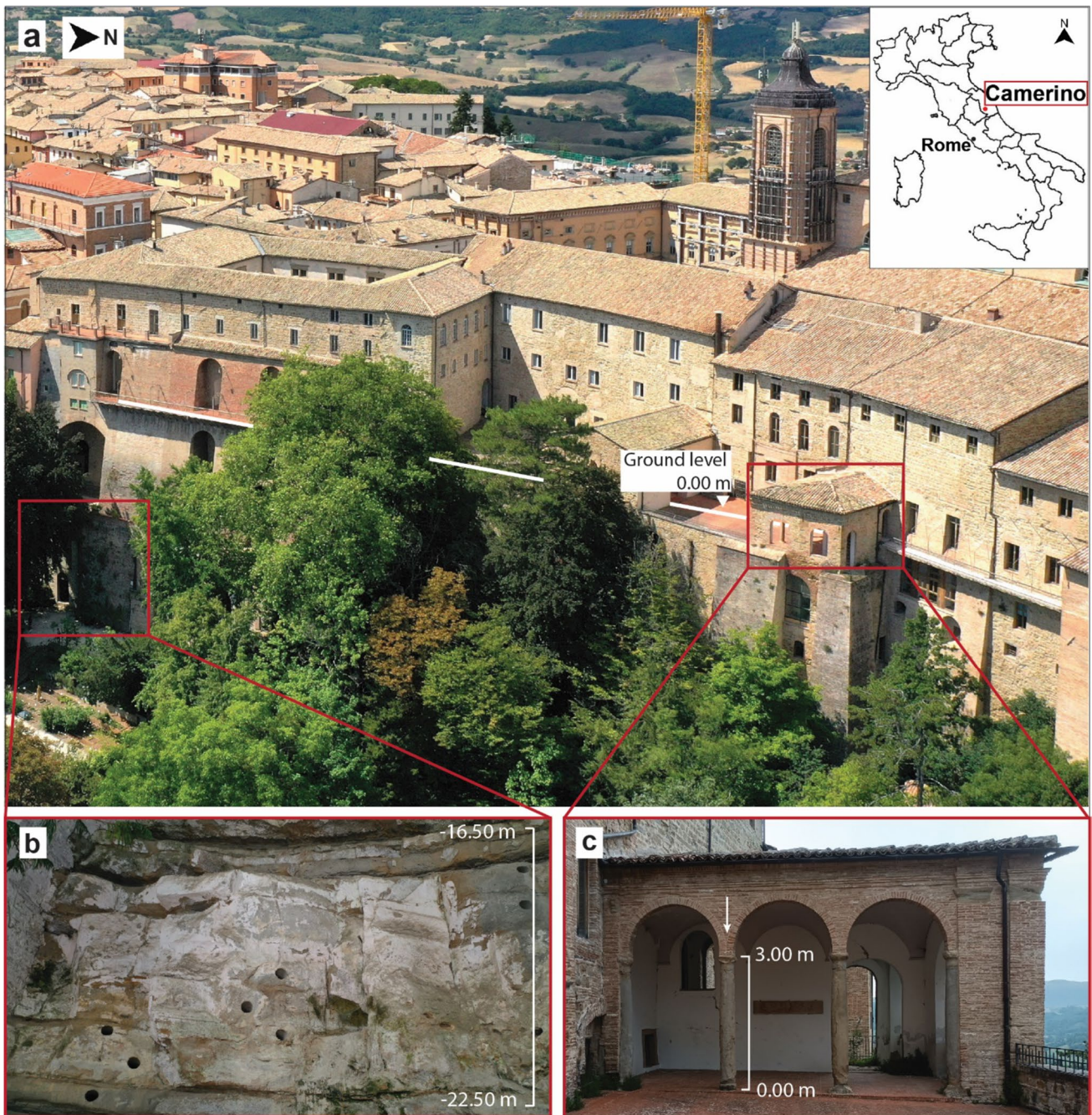
Fig. 1 **a** Aerial view of Palazzo Ducale in the historic town centre of Camerino (MC) with highlights of the study sites and indication of the ground level; **b** outcrop of the Orto Botanico of the University of Camerino with reference to the ground level; **c** small arcade of Palazzo Ducale with the indication of the analysed column with reference to the ground level

structure that includes multiple buildings, among which a small arcade consisting of four columns in total is located in the eastern side (Fig. 1c).

The arcade, as well as the palace, is entirely made of the sandstones of the Camerino Fm., as it was an easily available material both on-site and in the nearby quarries and used in almost all the architectural complexes of historical-artistic importance in the city (Frattali 1999). Palazzo Ducale (Fig. 1a) was completed in the second half of the fifteenth century in Renaissance style by order of the lord of the city Giulio Cesare da Varano (Paraventi 2003), and at the time, was considered one of the most sumptuous palaces in Italy. The sandstone columns of the small arcade are 3 m high and composed of a central monolith body, a capital and a base. The study was focused on one of the columns (Fig. 1c) in which previous data regarding the evaluation of the conservation state through mineralogical and petrographic analyses were available (Fig. 3a from Mattias et al. 1996). The sandstone outcrop of the Orto Botanico of the University of Camerino has been established as the provenance site for the columns of the palace, according to previous petrographic and geochemical investigations (Mattias et al. 1996) and for its proximity to the palace (Fig. 1b).

The sandstones of the Camerino Fm. are typically grey with occasionally ochre-brown halos. The grains are both rounded and angular with grain size ranging from 0.1 to 0.4 mm (very fine to medium sands). According to Folk's classification system (Folk 1974), these sandstones can be classified as greywackes or lithic arenites, based on their textural maturity. In Fig. 2, thin sections made from flakes collected in the columns of the arcade show (in order of abundance) quartz, carbonates and spathic calcite, lithic fragments, Na-Ca and K-feldspars with varying degrees of alteration, biotite with frequent oxide inclusions, chlorite and rare pyrites; calcite cement and clayey matrix with fossil elements are also present.

Weathering state

The columns of the small arcade of Palazzo Ducale are characterised by an extensive heterogeneous alteration (Fig. 3), as documented by photographs taken in the 1980s of the last century (Fig. 3a) and in the capitals (Fig. 3b), while sandstone crumbles and breaks up in loose sand in the columns' base, leading to considerable loss of stone material (Fig. 3c). Flakes and scales of several millimetres thick can deepen and expose the underlying rock layer as the phenomenon reaches an advanced stage (Fig. 3d). Significant discolouration (Fig. 3e) and vertical fissures (Fig. 3f) can also be observed.

Mattias et al. (1996) provided a complete mineralogical and petrographic characterisation of the lithic elements of the building, giving an indication of the state of preservation and/or possible causes of alteration of these sandstones; the authors stated that the masonry blocks of the palace, as well as the columns, are characterised by (a) a markedly high degree of oxidation with micro- and macroscopic halos of iron oxides; (b) dissolution and precipitation processes affecting $CaCO_3$ leading to the formation of gypsum; and (c) a relatively high content of halite derived from historical archives of salt located in the Palazzo Ducale basement.

Materials and methods

The experimental investigations in this study were carried out both in situ and in the laboratory. The in situ investigation consisted of a grain size analysis coupled with Equotip hardness testing, a non-destructive rebound-based device innovatively used to characterise both surface and in-depth hardness. This data collection was aimed at detecting hardness variation on the column surface, to assess possible relationships among surface hardness and grain size and to evaluate the change of hardness with depth. Moreover, to correlate surface hardness variation with physicochemical and mineralogical changes of

Fig. 2 Microscopic features of the sandstone of the Camerino Fm. derived from flakes collected from the columns of the small arcade of Palazzo Ducale: **a** Plane-polarised light; **b** cross-polarised light. Q, quartz; C, calcite; B, biotite; Lf, lithic fragments; F, feldspar
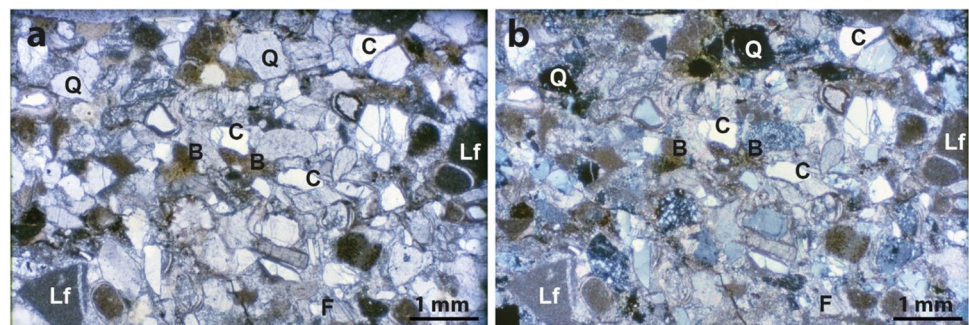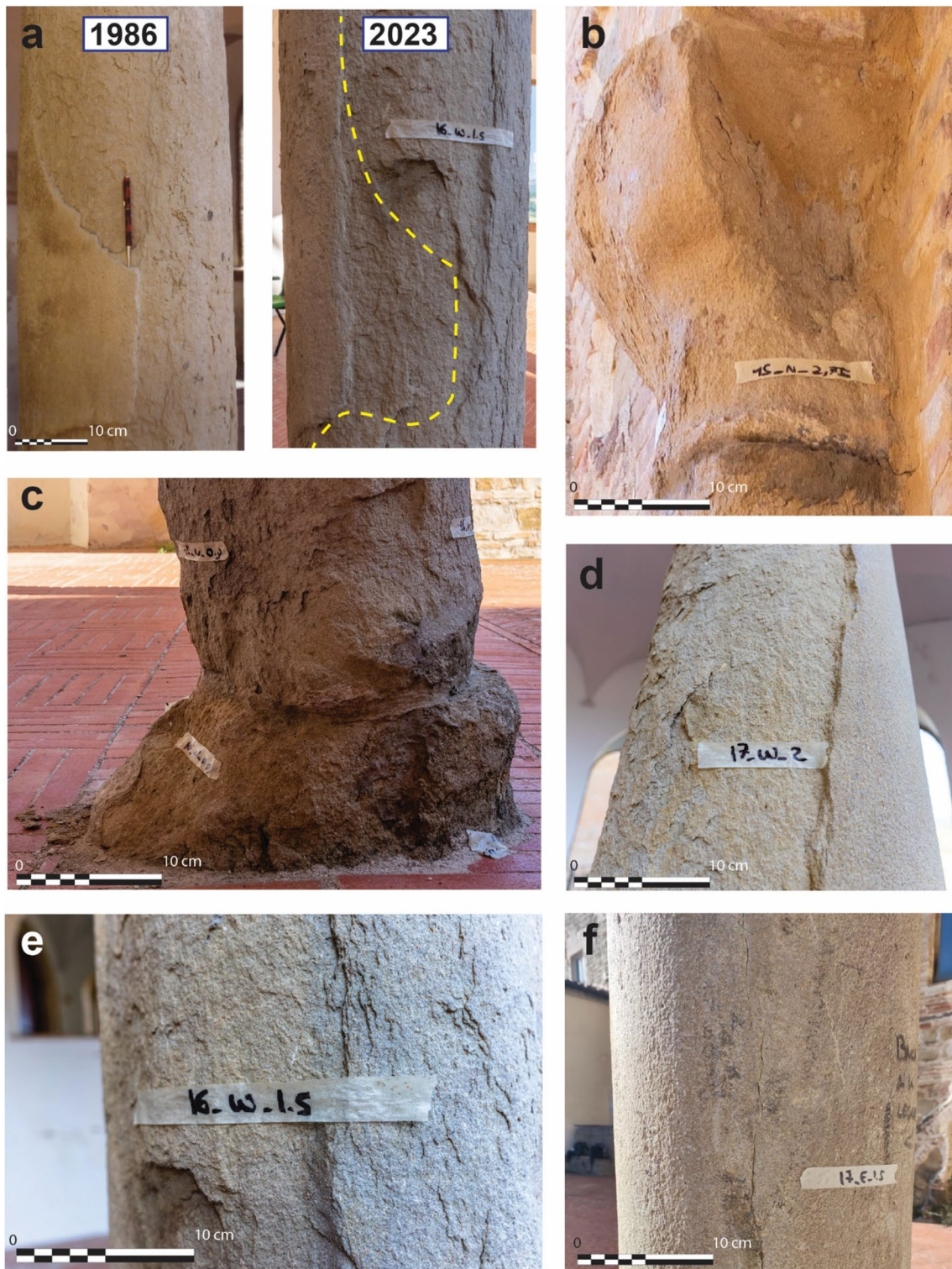
Fig. 3 Evidence of the sandstone's degradation in the columns of the small arcade of Palazzo Ducale: **a** loss of stone material from 1986 (modified from Mattias et al. 1996) to 2023; **b** detachment of large volumes of rock in the capitals; **c** granular disintegration and crumbling in the base; **d** scales and flakes exposing the underlying rock layer; **e** discolouration; **f** vertical fissures (fracturing)

the altered sandstone, small flakes (naturally detaching from the column surface) were collected and analysed through mercury intrusion porosimetry, scanning electron microscopy and X-ray diffractometry methods. The data collection was set up considering areas with different colours within the column, which can be a first indication of the weathering distribution. Mineralogy, texture and pore size distribution were correlated with the mechanical parameters, and a comparison with the intact rock from the outcrop (Fig. 1b) was made. Since Palazzo Ducale is a site protected by the Superintendence of Cultural Heritage, the data collection strategy proposed allows respect for the rules for protected sites.

Equotip hardness testing (EQ)

A compact version of Equotip (EQ model Piccolo 2, produced by Proceq, Switzerland) has been selected for the in situ evaluation of the sandstone hardness. EQ is a small electronic spring-loaded device that has been originally developed for metals, but is also increasingly used for rock hardness (Kawasaki et al. 2002; Kompatscher 2004; Aoki and Matsukura 2007; Viles et al. 2011). This device is easy to handle due to its small size and weight (only 142 g) and is based on a spherical tungsten carbide test tip mounted in an impact body which, thanks to the spring force, rebounds against the surface to be tested (Proceq© 2010) (Fig. 4a). The EQ hardness value is expressed as the "L" index (Leeb number) and is calculated by the ratio of the rebound velocity to the impact velocity multiplied by 1000 (Leeb 1979). Low rebound values indicate soft, porous and/or weathered stone surfaces, while higher values are indicative of less weathered or hardened surfaces (Wilhelm et al. 2016). Innovatively, two different EQ probes available from Proceq© (2010) have been used: the standard D (Fig. 4b) and the DL probe (Fig. 4c). The D probe is used for surface measurements and has a small impact body (27 mm) measuring 3 mm in diameter. In contrast, the DL probe, commonly adopted to access tight spaces and hard-to-reach surfaces, has a slim long front section (82 mm) and a slightly smaller diameter end (2.78 mm). In this study, the DL probe was innovatively involved to evaluate the hardness of the internal portion of the rock.

Both single (SIM) and repeated impact test methods (RIM) were used in conjunction (Aoki and Matsukura 2007, 2008; Yılmaz 2013; Wilhelm et al. 2016; Desarnaud et al. 2019; Mammoliti et al. 2021) to investigate the most superficial thin layer of the column (applying the SIM) and the deeper portion (applying the RIM).

SIM consists of collecting single impacts at different points, separated at least by a plunger tip (Aoki and Matsukura 2007), while RIM consists of consecutive impacts in a single point (Aoki and Matsukura 2008). According to Çelik and Çobanoğlu (2023), at least ten single impacts evenly distributed on a surface are recommended for an adequate investigation while, regarding RIM, repeated impact values at one point can cause the hardness value to be obtained incorrectly in a polymineralic stone (Çelik and Çobanoğlu 2019). This issue was

Fig. 4 a Schematic drawing of the EQ model Piccolo 2; b standard D probe; c DL probe
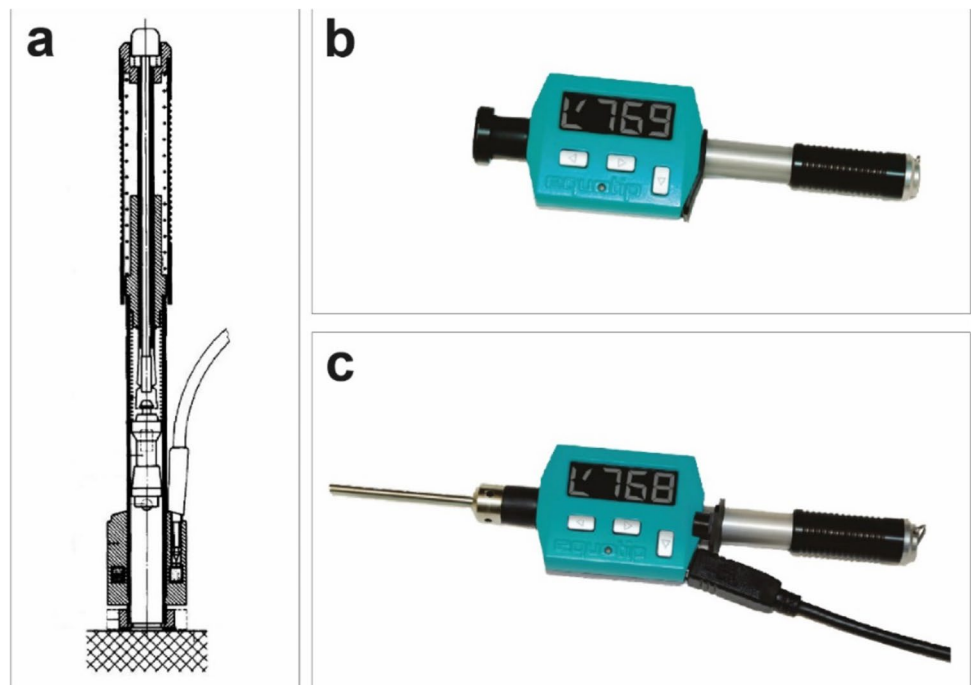
avoided by applying the RIM on ten different points in a small investigation area (about 10×10 cm), collecting 40 repeated impacts for each point and computing the average value discarding the first ten measurements (Mammoliti et al. 2021). In addition, SIM was employed for the calculation of the k-value parameter (Aoki and Matsukura 2007), used to determine the hardness of fresh and weathered superficial portions of rocks displaying a thin weathering layer, as follows:

$$k \text{ value} = \frac{L_s}{L_{max}}$$

in which L_s is the average of the ten values collected with the single impact method and L_{max} is the average of the three largest rebound values of the repeated impact method. After calculating the k-value, RIM alone was considered for hardness investigation.

Weathering mapping and damage categories

The mapping of weathering forms is a systematic investigation proposed by Fitzner et al. (2003) and revised by the ICOMOS International Scientific Committee for Stone (ISCS) (Vergès-Belmin 2008) as a glossary on stone deterioration patterns. However, Fitzner et al. (2003) proposed a classification for stone weathering according to four groups of material weathering: (1) loss of stone material; (2) discolouration/deposits; (3) detachment of stone material; and (4) fissures/deformation. In turn, each group is subdivided into *main weathering forms* (e.g. back weathering, discolouration, flaking) to which an intensity grade was assigned by Fitzner et al. (2003). In this paper, only the "discolouration" parameter, different from what already proposed by Fitzner et al. (2003), was modified in two discolouration classes: "ochre" and "grey". Based on this classification of weathering forms and their intensities, six damage categories were defined by Fitzner and Heinrichs (2002) and Fitzner et al. (2003): 0 — no visible damage, 1 — very slight damage, 2 — slight damage, 3 — moderate damage, 4 — severe damage, 5 — very severe damage. A correlation scheme was developed by Fitzner and Heinrichs (2002) to relate all observed weathering forms — considering their type and intensity — to damage categories, determining damage categories separately for the four groups of weathering. In the following step of evaluation, a final scheme was elaborated to obtain the final damage categories jointly considering all groups of weathering forms.

In this study, the correlation scheme of Fitzner et al. (2003) was adapted for the sandstone column of the small arcade of Palazzo Ducale, in which the observed damage categories were related to the EQ rebound.

Grain size analysis

Grain size analysis was carried out in the sandstone column to investigate the effect of grain size on the surface mechanical properties of the rock. For this purpose, a tool called Macro-photo was specifically developed in this work. This tool consists of a bell-like cover with an external handle (Fig. 5a), white LED lights inside and a transparent grain size scale pasted in the wider part (Fig. 5b), which is the one that will fit onto the surface to be investigated. The reflex camera (Nikon D3200) is placed in the narrower part (Fig. 5a). This tool can be applied also to semi-planar or non-smoothed surfaces (like columns, precisely — Fig. 5c), thanks to a soft plastic edge that fits as well as possibly the irregular surface (Fig. 5b).

In order to obtain standardised and high-quality pictures (Fig. 6a, b), the internal LED light (Fig. 5b) reduces external noises such as sunlight or artificial lighting (Fig. 5c). The characterisation of the sandstone spot is then implemented through an Excel calculation sheet to identify sedimentological properties through multiple visual comparison scales for grain size, sorting, roundness and sphericity indexes. The Macro-photo method has been validated by performing a grain size analysis on digital photos of thin sections (Fig. 6c, d) using the JMicroVision software (Roduit 2019), in which the grains' longest visible axes (red lines in Fig. 6c) were measured and used to compute the statistics for each grain size class (Fig. 6d).

Mercury intrusion porosimetry (MIP)

Not only the chemical and mineralogical composition but also the microstructure is determinant in rock weathering (Török et al. 2007; Labus and Bochen 2012). Therefore, the microstructure of stone in terms of total porosity and pore size distribution were investigated by mercury intrusion porosimetry (MIP) using a PASCAL 240 (Thermo Fisher Scientific, Waltham, MA, USA) porosimeter and a macropore analyser (Carlo Erba Instrumentation Series 12) with a measuring pressure ranging from 0.01 to 200 MPa. For each type of stone, three scales at least 0.5 cm thick were selected and tested, and the average results were reported. According to the test range of the porosimeter, total open porosity and pore size distribution were obtained for pore sizes between 0.0070 and 116 µm.

Mineralogical investigation

X-ray diffractometry (XRD)

In order to determine the mineralogical composition of the samples studied and to verify if different mineral phases could justify the different colourations of sandstone observed in the

Fig. 5 Macro-photo tool employed in the sedimentological characterisation of the sandstone column: **a** bell-like cover with an external handle with camera placed on the narrower part of the tool; **b** LED lights inside the bell-like cover and transparent grain size scale pasted in the wider part of the tool; **c** application of the tool on the column, obtaining a high-quality picture (Fig. 6a, b) where to perform the grain size analysis

column and between the column and outcrop, X-ray diffractometry (XRD) was employed to identify and compare the mineralogical composition of the different sandstone specimens. Samples have been finely ground in an agate mortar and mounted in a brass sample holder by side-loading in order to minimise iso-orientation of the grains. A Philips PW 1830 diffractometer equipped with a Cu tube and a diffracted beam graphite monochromator was used. Diffraction spectra have been collected in the 2θ range from 3 to 70° in step scan mode, with 0.02° step and 2 s/step counting time. The data were interpreted by comparison of the Mineral Powder Diffraction File Databook.

Scanning electron microscopy (SEM)

The mineralogy of sandstone samples was further examined using a scanning electron microscope (SEM) Zeiss Sigma 300. The selected flakes from the column and a portion of the core sample were pre-consolidated and then incorporated in epoxy resin due to the fragile nature of the sandstone. Polished thin sections from the column and from the core samples were

realised and analysed. Petrographical information has been obtained as well as qualitative observations about porosity and pore filling; mineral alteration and oxidation; and elemental maps to highlight geochemical distribution.

Testing strategy

The testing strategy presented in this work consists of two successive phases, in which the first is aimed at assessing the influence of grain size on the EQ rebound and the second focused on fixed grain size zones where physicochemical and mineralogical analyses are performed and correlated with the EQ rebound. In the first phase (Fig. 7a, green dots), more than 900 impacts were collected with EQ D probe, following a systematic data collection at fixed heights (0.05, 0.3, 0.7, 1.5, 2.0, 2.75 m) and orientations (around the perimeter at 90° right angle, Fig. 7a), in which 24 measuring points (MPs) were distributed on the column surface. Twelve MPs (1–12) were placed on the side of the column facing south-west
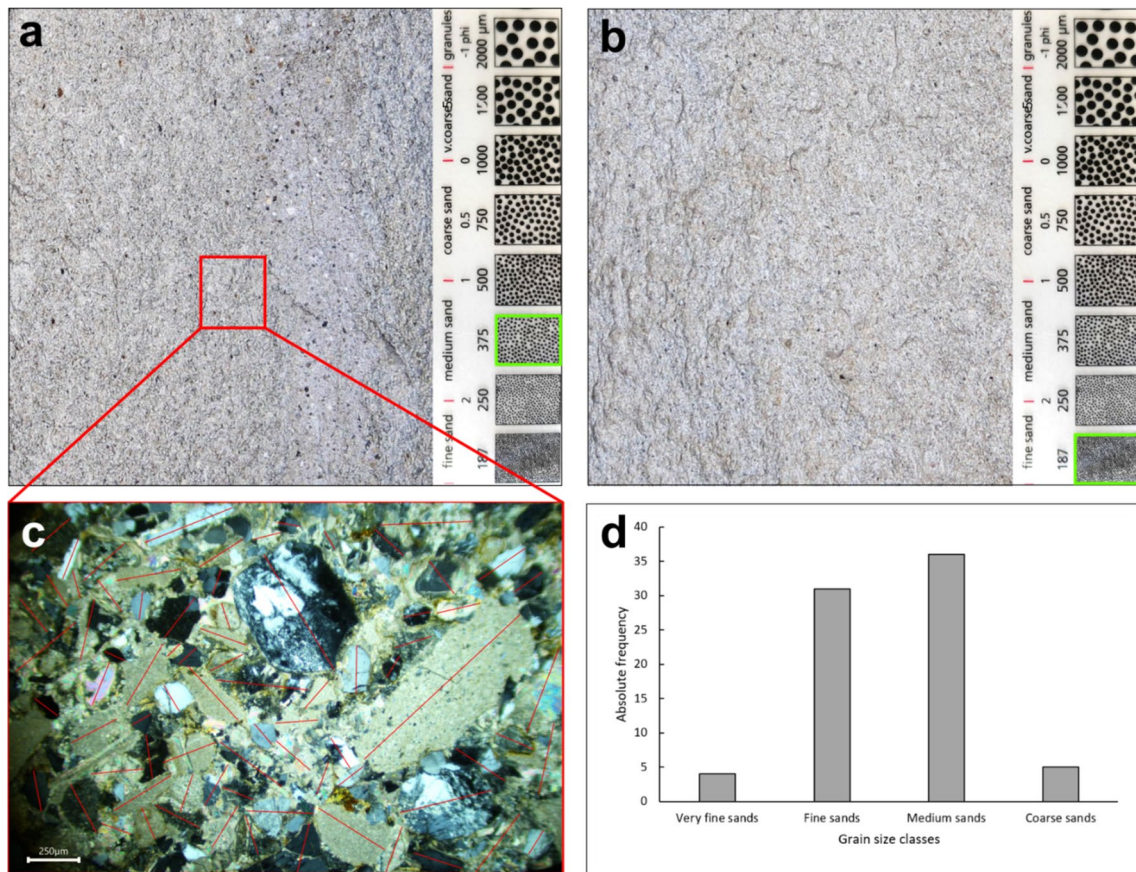
Fig. 6 Examples of grain size analysis in the column obtained with different methods: **a** medium sand and **b** fine sand obtained through the Macro-photo method; **c** validation of the medium sand evaluation through the JMicroVision software (cross-polarised light thin-section image); and **d** absolute frequency histogram of grain size classes relative to Fig. 6c

in the outer arcade, while the other 12 MPs (13–24) were placed on the side facing north-east and the inner arcade. For each MP, grain size was evaluated using the Macro-photo tool, and EQ data were collected using the RIM, by taking 40 consecutive EQ impacts at ten different points (Fig. 7a). To assess the change in hardness from surface to depth due to weathering, the DL probe was used in one MP using the RIM (Fig. 7a, green dot highlighted in yellow — MP18) on a hole of approximately 0.5 cm diameter and 3 cm depth on the column, made by power drill. Compressed air was used after drilling to avoid the accumulation of soft material at the bottom of the hole, which would have invalidated the EQ test. In the second phase of testing, heterogeneity in surface hardness was further investigated in six selected areas in the outer arcade exposure (pink circles in Fig. 7b), from now named "alteration zones". Alteration zones labelled A1, B1 and C1 refer to the ochre coloured zone, while A2, B2 and C2 refer to the grey one. Specifically, for each alteration zone, grain size was determined and EQ was applied using SIM and RIM at ten different points (Fig. 7b, pink circles). Afterwards, mineralogical and physical properties were investigated by MIP, SEM and XRD analyses on flake samples from zones B1 and B2 (Fig. 7b, striped, pink circles).

Eventually, a single core was selected from about 20 cores collected by Mammoliti et al. (2023) along the different strata of the sandstone outcrop of the Orto Botanico (origin site of the column following Mattias et al. (1996), Figs. 1b and 8), to perform MIP, SEM and XRD analyses. The core was extracted from a layer with a significant thickness (bigger than the column radius) and with the same grain size of the area in which MIP, SEM and XRD analyses are conducted in the column. Then, the selected core was cut to investigate the core's innermost portion (grey portion in Fig. 8), where mechanical tests were conducted to obtain the properties of the intact sandstones. In this case, the surface hardness was measured through the D probe, applying the RIM in two spots (Fig. 8, light blue dots), while the mineralogical (thin sections and XRD analysis) and physical analyses were performed on the core surface distinguishing the two coloured zones (grey and ochre, Fig. 8, dark green circles).
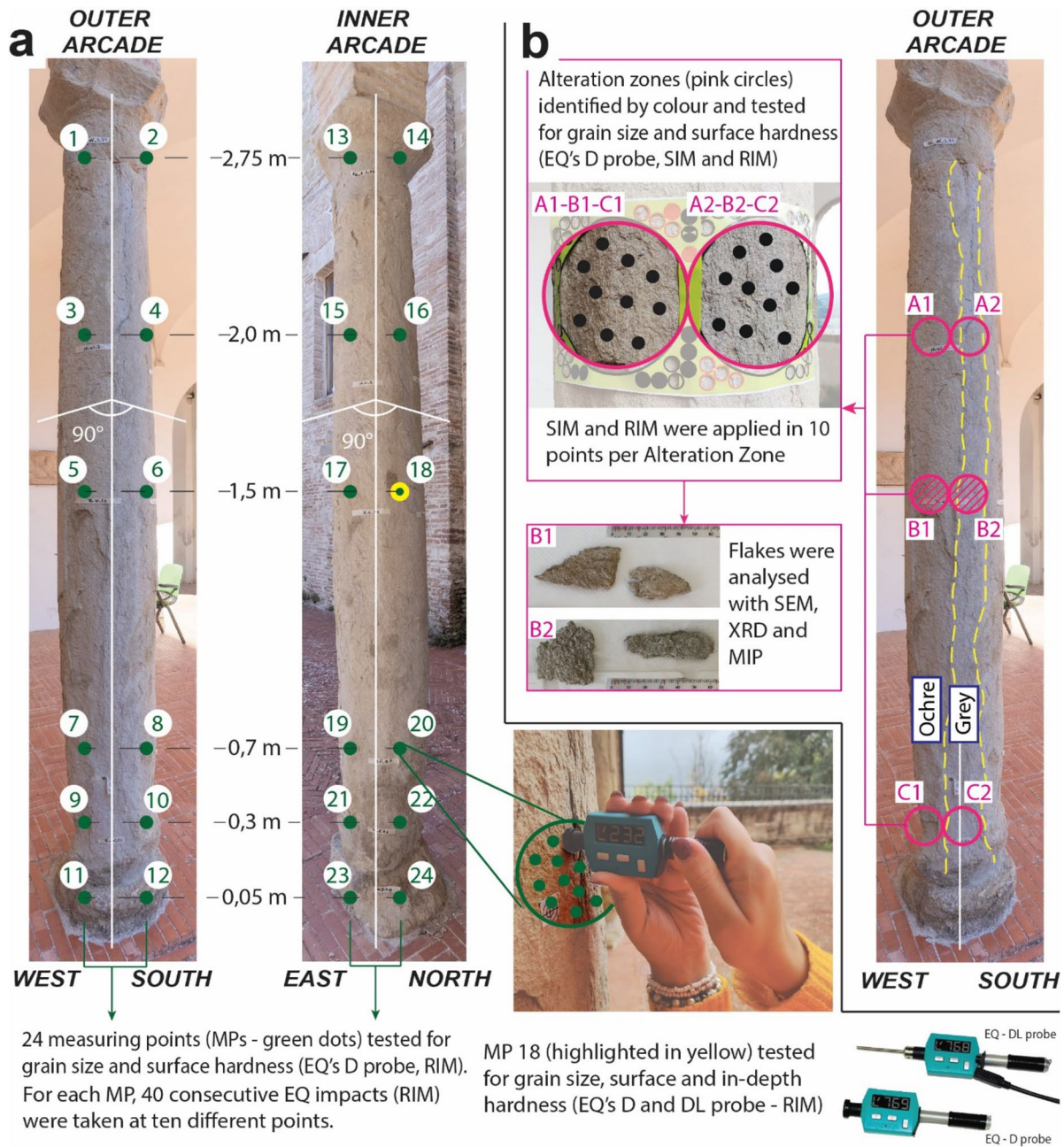
Fig. 7 Schematic representation of the testing strategy conducted with EQ, Macro-photo, SEM, XRD and MIP: **a** overview of the 24 MPs (green dots) placed in the outer and inner arcade exposure, where surface EQ data (D probe — RIM) and grain size were acquired. In-depth EQ probe (DL probe— RIM) was then employed in a single MP (green dot highlighted in yellow — MP18). **b** Alteration zones (pink circles) investigated with EQ (D probe — SIM and RIM) and Macro-photo. A1, B1 and C1 refer to ochre zone; A2, B2 and C2 refer to grey zone. Flakes for mineralogical and physical analyses were collected from B1 and B2 (striped pink circles)

Results

Damage categories vs. EQ

As reported in Table 1, only damage categories from 1 to 4 were found in the investigated column, while all four groups of weathering forms were detected. The terminology of the ICOMOS glossary (Vergès-Belmin 2008) and of Fitzner et al. (1995) was associated with the macroscopical observations carried out in the column. Specifically, back weathering and break out were observed on the column body and capitals (Fig. 3a, b), granular disintegration into sand and crumbling were detected on the column base (Fig. 3c), while contour scaling and flakes
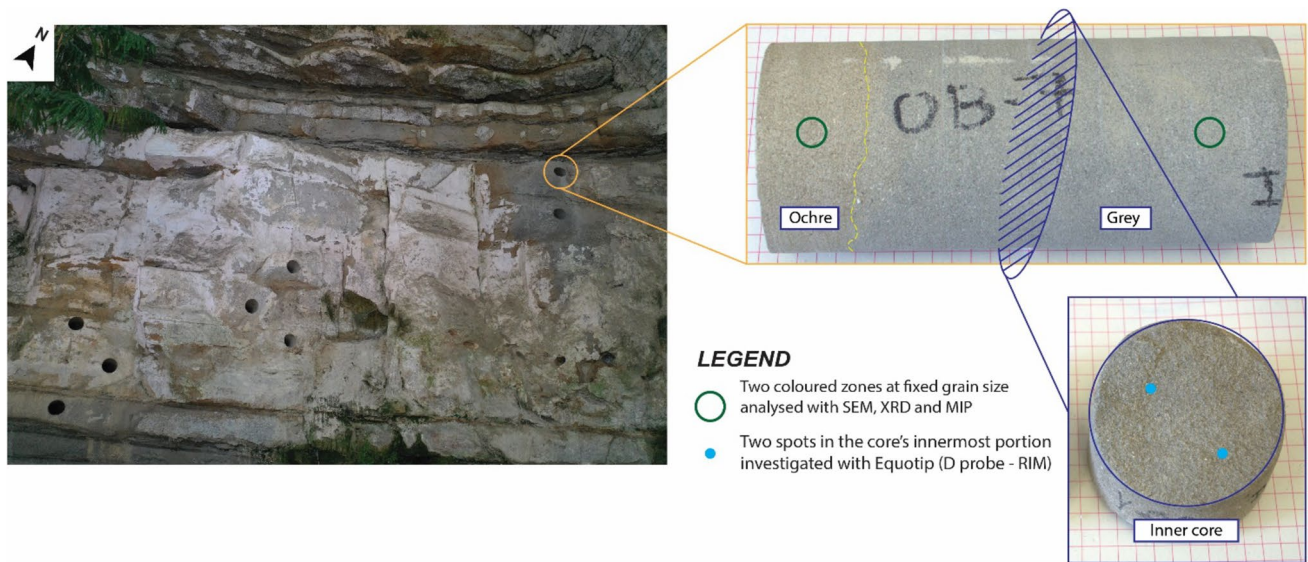
Fig. 8 Testing strategy in the provenance site (Orto Botanico outcrop), selecting a suitable core according to the thickness and grain size of the strata. EQ was employed in the core's innermost portion (D probe — RIM, light blue dots), while flakes were collected from the core surface and analysed with SEM, XRD and MIP, according to ochre and grey zones (dark green circles)

Table 1 Weathering forms and their intensities mapped according to the 24 MPs. Table modified from Fitzner et al. ([2003](#))

ARCHITECTURAL FEATURE	MEASURING POINT (MP)	1. LOSS OF STONE MATERIAL			2. DISCOLOURATION/DEPOSITS			3. DETACHMENT OF STONE MATERIAL						4. FISSURES	Damage Categ.	AVG EQ
		Back weathering	Relief/alveolar or rounding/notching	Break out	Discolouration *	Terrigenous deposits	Crusts	Granular disintegration into sand	Crumbling	Flaking	Contour scaling	Crumbling + Flaking + Contour Scaling	Detachment of crusts with stone material	Fissures		
BASE	11				Ochre	1	2				2				3	245.2
BASE	24			2	Ochre							3			3	269.2
BASE	23			2	Ochre							2	1	3	4	287.2
CAPITAL	14	2			Grey			2							3	293.8
BODY	22	2			Grey					2					3	305.3
CAPITAL	13		1		Grey										2	328.7
BODY	16		1		Ochre					2					2	354.8
BODY	10				Ochre					1	1				2	356.7
BODY	20				Grey					2					2	360.8
BODY	19				Ochre			1		1					2	366.8
CAPITAL	2				Grey						2				2	377.6
BODY	15		1		Ochre					1					1	391.1
BODY	9				Grey			1		1	2				4	401.6
BODY	17				Ochre			1							1	411.9
CAPITAL	1				Ochre					1	1				2	430.8
BODY	18		1		Ochre										1	431.2
BODY	7	2			Grey										2	441.6
BODY	21				Ochre										1	470.6
BODY	3				Ochre						1				1	481.8
BODY	8				Ochre					1					1	481.9
BODY	6				Ochre						1				1	502.9
BODY	5	3			Ochre						1				3	520.2
BODY	4				Ochre						1				1	537.3
BASE	12				Ochre	1									1	546.2

*Discolouration was applied in this study to the two individuated coloured zones: ochre and grey

are responsible for the detachment of large, platy stone elements, exposing the underlying rock layer (Fig. 3d). Instead, vertical fissures were detected in one MP only (Fig. 3e).

Subsequently, EQ hardness average values measured in the 24 MPs (located in the capital, body and base of the column) were associated with the damage categories (Table 1; Fig. 9a).

In general, low rebound data (240 < L average < 300) are measured in moderate/severe damage zones (damage category 3–4) in the base (west, east and north exposure) and in the capital (north exposure), the latter displaying a slight/moderate damage (damage category 2–3) in the outer arcade exposure. Conversely, the body of the column is characterised by a very slight/slight damage (damage category 1–2), combined with higher rebound values (350 < L
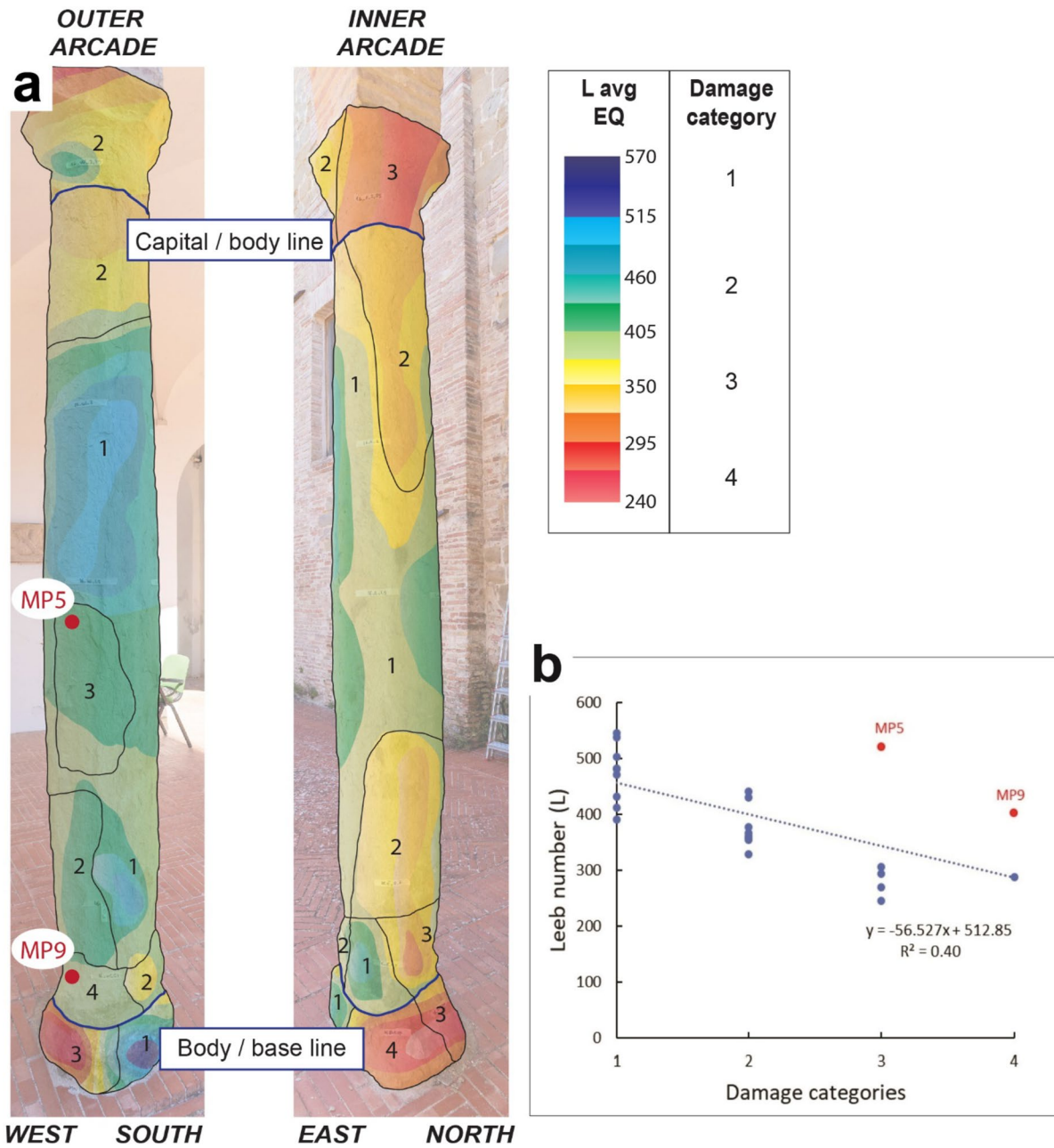
Fig. 9 **a** Distribution map of EQ average values measured in the 24 MPs and of the damage categories (damage categories from 1 to 4) found in the column; **b** Relationship between EQ rebound data and damage categories with evidence of the two outliers (MP5 and MP9, highlighted in red)

average < 420). The body of the column exposed to the outer arcade has the highest rebound values (L average > 500) and a low degradation category (damage category 1).

The relationship among EQ values and damage categories is reported in Fig. 9b, where a negative linear association ($R^2 = 0.40$) is shown. However, few outliers (highlighted in red in Fig. 9) are observed for damage categories 3 and 4. In fact, in MP9 (Fig. 9a), a high damage is observed and EQ displays high rebound values. The presence of these outliers may be attributed to the inherent heterogeneity of sandstone, coupled with the orientation of the specimens. Notably, both outliers are placed in the MPs with west exposition (MP5 and MP9 respectively). This suggests that the spatial alignment of the samples may play a role in the observed extreme EQ values for categories 3 and 4 and may be one of the countless parameters influencing the mechanical behaviour of sandstone.
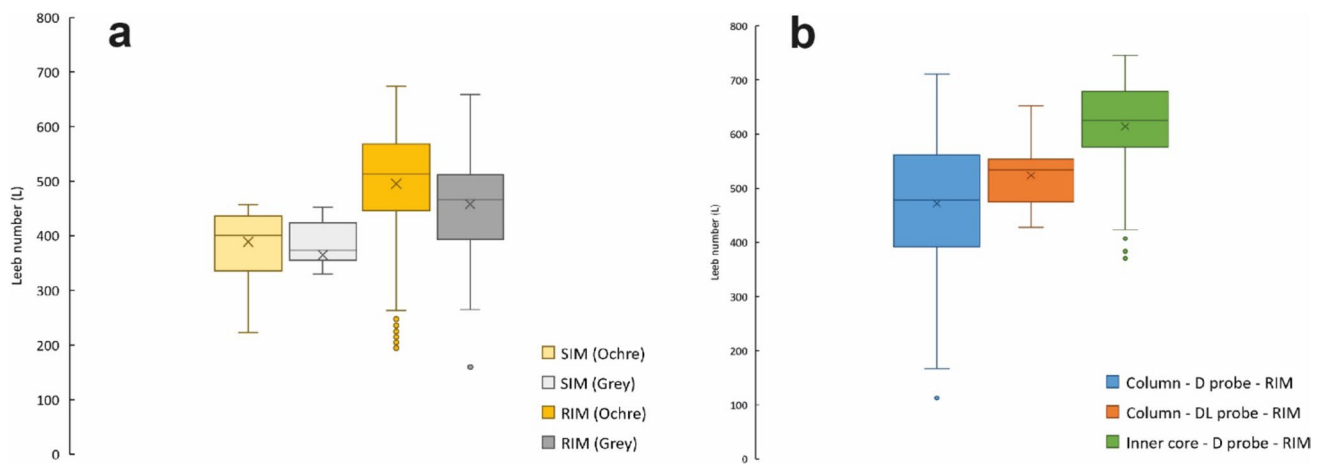
Fig. 10 Box plots of the EQ results: **a** SIM and RIM for each coloured zone; **b** surface measurement with the D probe carried out in the column (blue box), measurement at 4 cm depth with the DL probe (orange box), surface measurement with the D probe on the rock core (green box)

Table 2 Statistical data of the plots shown in Fig. 10b. RIM method was applied

	Column — D probe	Column — DL probe	Inner core — D probe
L min	113	428	371
L average	472	524	614
L max	711	652	746
St. dev.	113.9	56.3	81

EQ hardness testing

Applying the collecting data strategy presented in this work, consisting of 24 MPs equally distributed within the column, significant differences in surface hardness values were detected (Fig. 9a). In detail, categorising the data based on the colour (ochre and grey) and based on the impact strategy (SIM and RIM) (Fig. 10a), lower EQ values were observed for SIM with respect to RIM. SIM presents an average value of 389 L in the ochre part and 365 L in the grey one in contrast to RIM, standing between 423 and 521 L. In addition, the ochre colour was characterised by higher values in respect to the grey colour, under the same impact method. In Fig. 10b, rebound data acquired with the RIM in the column surface using the D probe (blue box) were plotted with data at 4 cm in depth acquired with the DL probe (orange box) and with surface data of the core sample (green box – D probe). In this way, the surface and in-depth hardness data of the column can be compared with those of the provenance site rock. The results (Table 2; Fig. 10b) clearly showed a considerable hardness reduction from the column surface (blue box — EQ D probe, RIM, L average = 472) to the core of the Orto Botanico outcrop (green box — EQ D probe, RIM, L average = 614). Moreover, examining the change of

EQ values from column surface (blue box in Fig. 10a) to 4 cm depth (orange box — DL, RIM, L average = 523), an increase of the EQ can also be observed. A general higher variability of the EQ data on the column surface was demonstrated by the highest standard deviation (st. dev. = 114) (Table 2).

The data acquired on the core drilled at the Orto Botanico outcrop were assumed to be the reference rock values (fresh rock). Based on this assumption, the degree of surface alteration, expressed by the hardness reduction (in percentage) from 4 cm in depth to the surface, amounted to 10%, while the hardness reduction of the column surface compared to fresh sandstone reached 25%. This indication was also confirmed by the k-value, calculated with the approach of Aoki and Matsukura (2007). In fact, the k-value parameter for the provenance site is 0.73 whereas the k-value calculated in the column is 0.59 and 0.56 for the ochre and grey zone, respectively, evidencing a hardness reduction from the outcrop site to the surface of the column, in which the ochre zone is harder than the grey zone.

Grain size vs. EQ

Three granulometric classes have been found through the Macro-photo technique: "very fine sand", "fine sand" and "medium sand" (Figs. 5 and 6). These grain size classes are differently distributed along the column (Fig. 11), with the most recurrent grain size class represented by the "fine sand" (18 MPs out of 24 MPs), followed by "medium sand" (4 MPs) and "very fine sand" (2 MPs). EQ data collected in the whole dataset (24 MPs) for each granulometric class has been tested using the one-way ANOVA test (Fisher 1970) (Fig. 12a). The results highlighted that the granulometric classes are statistically different (p-value < 0.05), with the fine grained sand displaying the lowest values
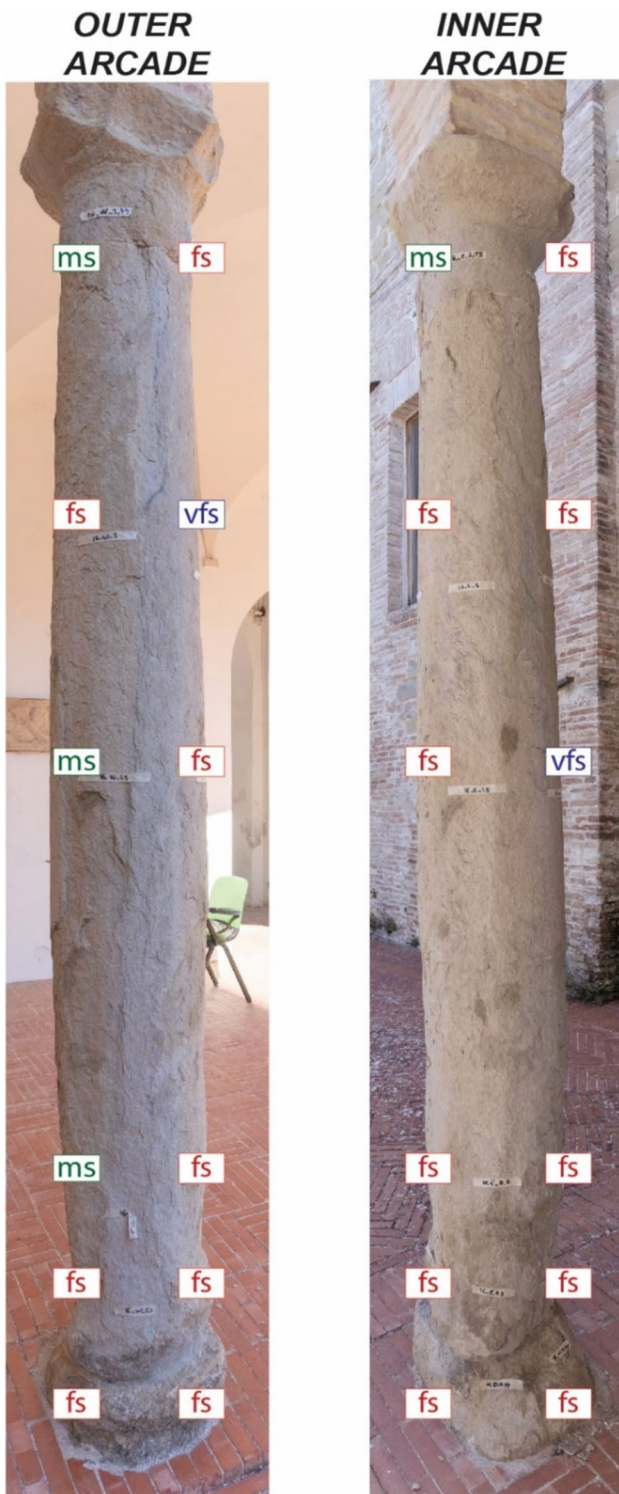
Fig. 11 Grain size distribution along the 24 MPs in the column's surface: vfs, very fine sand; fs, fine sand; ms, medium sand

size; this is not the case for very fine sand, which show the highest values, not following a trend with grain size. The ANOVA test has been also applied to two selected alteration zones (pink striped circles labelled B1 and B2 in Fig. 7b) of the same grain size class (medium-grained sand) and categorised based on the colours (grey and ochre); the test (Fig. 12b) demonstrated that the two groups are different with statistical significance (p-value < 0.05).

Porous system in medium-grained sands

Table 3 and Table 4 show the results of the MIP analysis performed on flakes from medium-grained granulometry of the column (Fig. 7b, pink striped circles, numbered B1 and B2) and from the core surface of the Orto Botanico outcrop (Fig.8, dark green circles) for both ochre and grey zones.
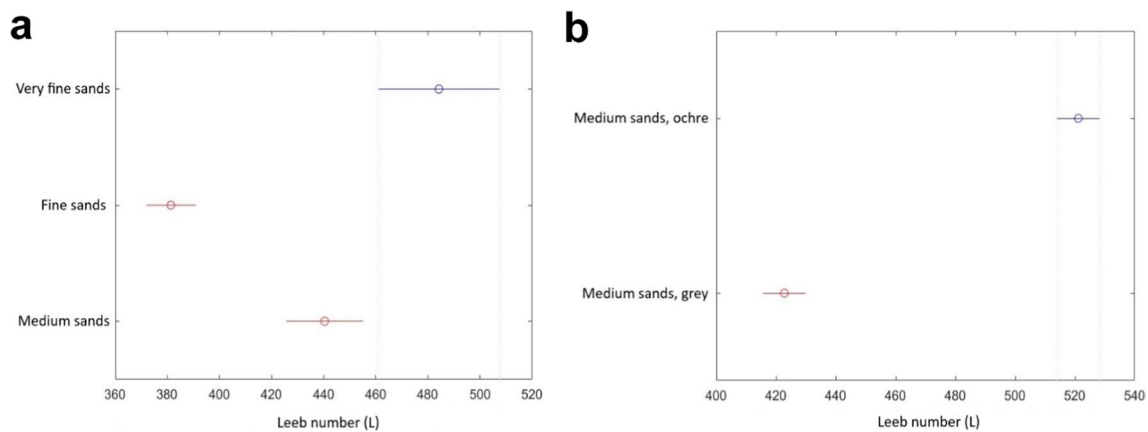
The four samples were characterised by a similar total open porosity (about 11%). However, the relative pore volume distribution, obtained by the derivative of the cumulative pore volume curve, of the column (for both colourations in Fig. 13) is significantly shifted towards bigger pores, as mesopores and macropores, than that of the core surface of the Orto Botanico outcrop (both ochre and grey colour). In particular, in the column, the pores were placed mainly in the 1- to 100-µm range (meso- and macropores), with mesopores more predominant in the ochre zone than in the grey one (47% vs. 35%) and macropores more abundant in the grey zone than in the ochre one (47% vs. 38%). On the contrary, about 80% of the porosity of the core samples was placed in the 0.1- to 1-µm range (micropores), with only 3–5% of macroporosity.

The results obtained by mercury intrusion porosimetry agreed with the observations of the porosity of the Orto Botanico core samples (Fig. 14a) and of the column ones (Fig. 14b) carried out by SEM. At 1000 magnification, only the bigger pores could be detected in the core samples since they rarely exceed 3 µm in diameter and they were also isolated from each other (Fig. 14a). Differently, in the column, the pores had quite different morphology, not circular but irregular or elongated shape that seemed to be caused by dissolution processes and union of multiple cavities (Fig. 14b).

However, the similar chemical composition, as subsequently reported in the "Mineralogy of the medium-grained sands" section, and the comparable total open porosity (about 11%) of the four specimens, even if shifted at bigger pores in column specimens, suggest that sandstone dissolution processes in the column have been followed also by chemical re-precipitation ones.

Mineralogy of the medium-grained sands

The XRD analysis performed on samples collected from the column surface (Fig. 7b, pink striped circles labelled B1

(L average ≈ 380), followed by the medium grained (L average ≈ 440) and very fine grained (L average ≈ 485 L) (Fig. 12a). Based on the test results, both fine and medium-grained sand showed higher EQ values with increasing grain

Fig. 12 **a** ANOVA test results for EQ tests in the 24 MPs, according to grain size classes; **b** hardness datasets plotted with medium grain size in the two selected alteration zones (pink striped circles, Fig. 7b)

Table 3 Total open porosity of the four samples analysed

Sample	Column — ochre	Column — grey	Core surface — ochre	Core surface — grey
Total open porosity (%)	10.1	11.2	10.3	10.4

Table 4 Pore diameter distribution, classified as micropores, mesopores and macropores, for the four samples analysed

Sample	*0.01–1 μm (micropores)*	*1–10 μm (mesopores)*	*10–100 μm (macropores)*
Column — ochre	15	47	38
Column — grey	18	35	47
Core surface — ochre	81	16	3
Core surface — grey	76	19	5

and B2) confirmed the mineralogical characterisation of the altered lithic elements provided by Mattias et al. (1996) in the columns of Palazzo Ducale. XRD results indicated that calcite and quartz were the most abundant phases (ca. 2:1 ratio), while plagioclases, K-feldspars (microcline and orthoclase) and phyllosilicates (mostly halloysite-7Å, kaolinite and muscovite/illite) were subordinated. Gypsum was present in minor amounts. No significant mineralogical differences were detected between weathered sandstone from the columns and the cores from the outcrop nor either between the grey and ochre zones of the column (Fig. 15).

As a result, the SEM analysis identified different stages of pyrite oxidation by means of the chemical distribution maps of sulphur (S) and iron (Fe). Figure 16 highlighted the different phases of the pyrite oxidation in either the core

sample (Fig. 16a), the grey zone of the column (Fig. 16b) or the ochre colour of the column (Fig. 16c), from low to high degree of alteration. In detail, Fig. 16c shows the almost complete oxidation of pyrite (still present in relict cores) with the formation of abundant goethite; goethite as an alteration product of pyrite has been identified thanks to the presence of a peak at 389 cm^{-1} in the RAMAN spectra of few representative samples. This assemblage is observed mostly in the ochre zones, whereas in the grey zones, pyrite is mostly unaltered. The process of pyrite oxidation is responsible for the formation of goethite and for the release of sulphur (possibly as sulphate) in solution. Apart from the pyrite oxidation, neither SEM data indicate any sensible differences in the mineralogy between the grey and ochre zones or between intact and altered samples.

Eventually, the results of SEM analysis performed in the column ochre zone revealed the presence of case-hardened zones (Fig. 17a, marked by yellow dashed lines). In these hardened zones, a high concentration of calcium (Fig. 17b, high calcium peak), precipitated from the oxidation of pyrite and subsequent release of sulphur into solution, was detected. The re-precipitated $CaCO_3$ partially occluded the pores, causing a decrease in macroporosity in the ochre zone compared to the grey one, as evidenced by MIP analyses (Table 4; Fig. 13).

Discussion

The methodological approach proposed in this paper is aimed at characterising sandstone alteration mechanisms in a column of a building protected by the Superintendence of Cultural Heritage in Central Italy, coupling a non-destructive approach based on the EQ hardness tester with grain size, MIP, SEM and XRD analyses. The comparison
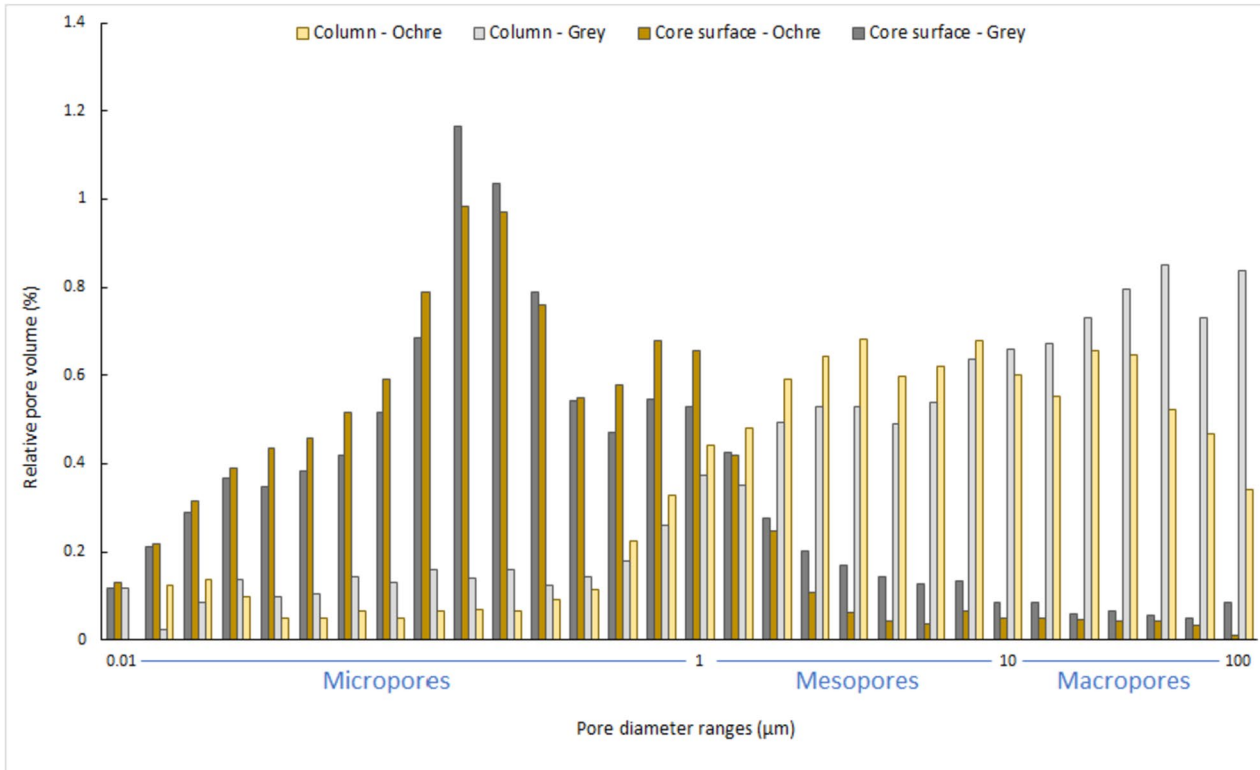
Fig. 13 Relative pore volume (%) distribution obtained by mercury intrusion porosimetry for the four samples analysed
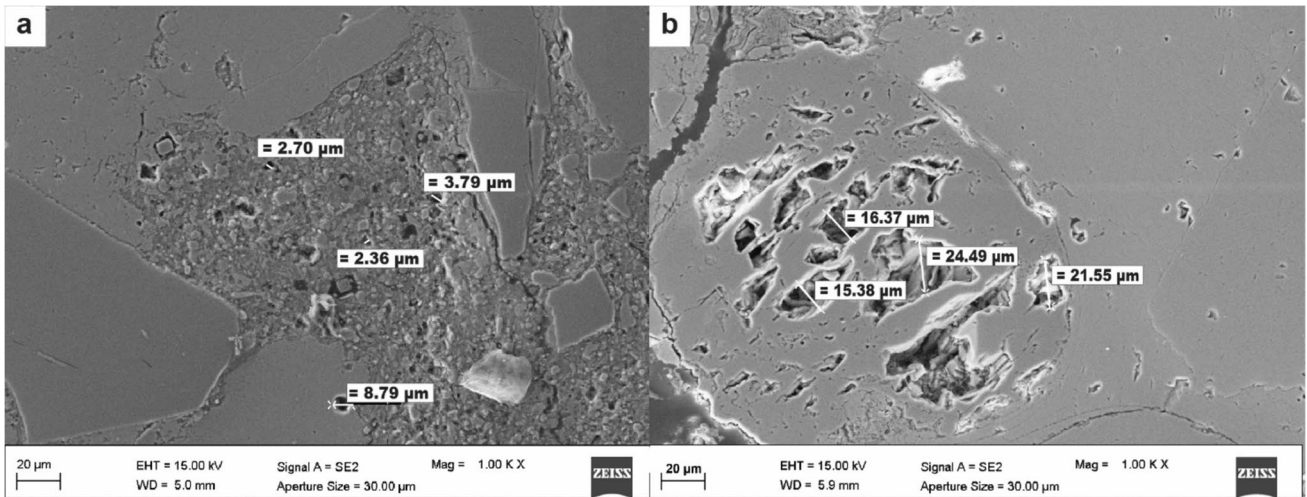

Fig. 14 SEM images acquired on representative samples from the outcrop and from the column: **a** round, isolated micropores in fresh sandstone cores; **b** irregular or elongated macropores in altered sandstone in the column

of the different techniques and the huge amount of rebound data (more than 900 impacts in 24 MPs) allowed to assess weathering heterogeneity within the same artefact. The effect of the natural variability of rocks on EQ data is quite known in the literature (Aoki and Matsukura 2008; Feal-Pérez and Blanco-Chao 2013; Wilhelm et al. 2016),

and such variability is likely to increase as weathering progresses (Wilhelm et al. 2016). The proposed collecting data approach with the EQ's D probe has proved efficient in detecting surface hardness heterogeneity. In fact, the EQ spatial distribution in the column was efficiently correlated with the damage categories derived from Fitzner et al.
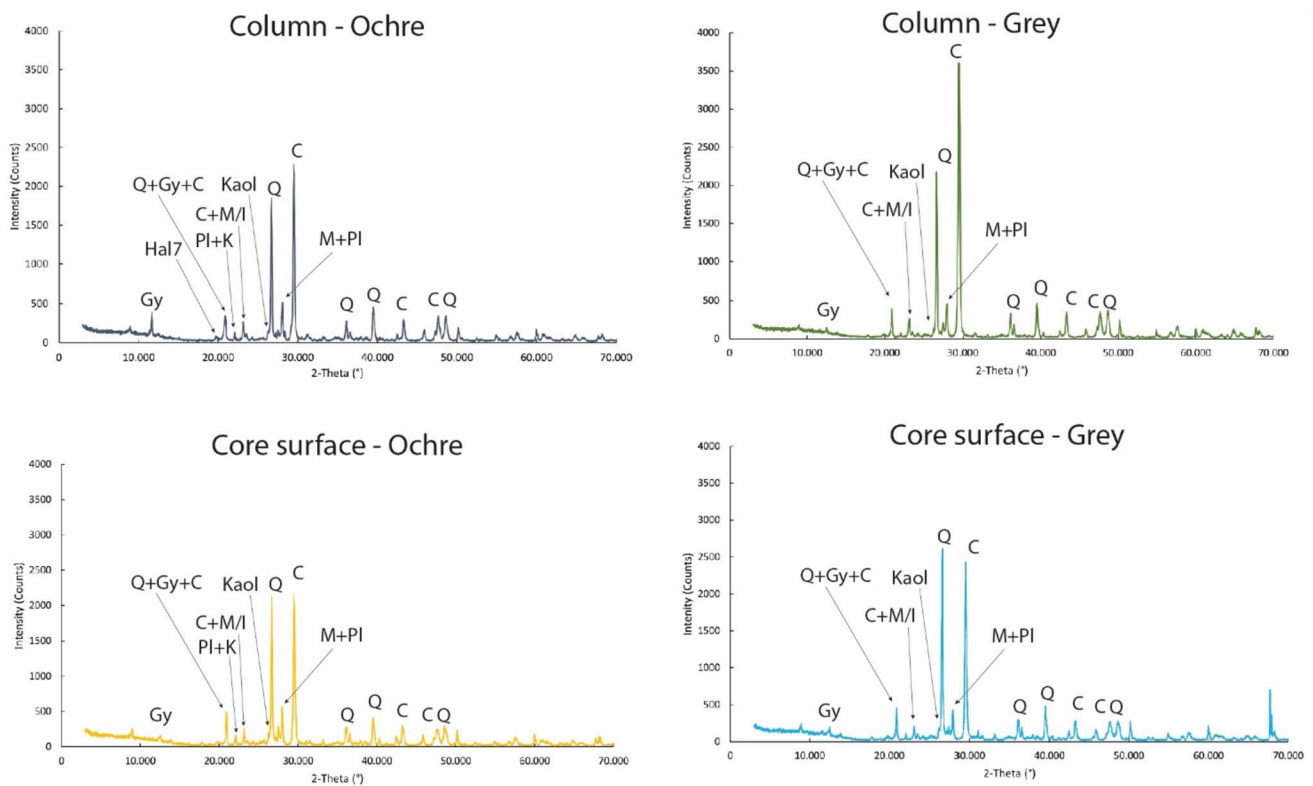
Fig. 15 XRD spectra of the column and core samples for the ochre and grey zones highlight similar mineralogic composition for all four samples: C, calcite; Q, quartz; Pl, plagioclase; Gy, gypsum; Hal7, halloysite-7Å; Kaol, kaolinite; M/I, muscovite/illite

(2003) (Fig. 9a); this evidence was in line with field observations (Fig. 3), in which sandstone degradation is represented by loss of materials, granular disintegration, crumbling, discolouration and the formation of vertical fissures. The reduction in hardness due to weathering was additionally assessed using the *k*-value of Aoki and Matsukura (2007) and by applying the SIM and RIM to the column surface. An innovative feature of this paper was the combined use of EQ's D and DL probes in the column, in comparison with EQ measurements on the rock core drilled in the provenance site (fresh rock), which provided a comprehensive overview of the reduction in mechanical strength caused by alteration. Moreover, the results showed that grain size has an effect on EQ rebound (statistically tested with ANOVA test), although only a small difference in mean EQ values is noticeable, with the coarser classes completely absent. The limited variability of the grain size classes and the absence of the coarser classes in the analysed column (ranging from very fine to medium sands) do not allow further consideration of the relationship between grain size and surface hardness. Therefore, this aspect may inspire further investigation/studies on the influence of grain size on rebound-based devices such as EQ. In fact, to our knowledge, the relationship among grain size distribution and the mechanics of clastic sediments remains generally controversial in the scientific

literature and is generally assessed using destructive UCS tests instead of rebound-based techniques. In detail, both negative (Fahy and Guccione 1979; Singh 1988; Shakoor and Bonelli 1991; Qi et al. 2022) and positive (Meng et al. 2006; Soroush 2008; Kong et al. 2021) associations among UCS and grain size have been reported while our use of rebound data introduces a novel dimension to this debate.

By focusing on the EQ testing in the ochre and grey zone in the medium-grained sands, higher Leeb values observed for the ochre zone were also supported by the MIP analysis results. In the column, mesopores were predominant in the ochre zone with respect to the grey (47% vs. 35%), while macropores were more abundant in the grey zone (47% vs. 38%). The discrepancy in EQ values in the column can initially be explained by the 10% difference in macropore volume between the ochre and grey zones (Table 4), with higher EQ values in the ochre than in the grey (mean 521 to 423 L, st. dev. 118 to 85). As reported by Huang et al. (2022), during weathering, many micropores (0.01–1 μm radius) can expand and interconnect, and then develop into macropores under freeze-thaw cycles. This condition is often found in rocks with a high volume of pores with a radius of < 1 μm (Çelik and Sert 2020).

In the fresh sample of the Orto Botanico outcrop, approximately 80% of the pores are classified as micropores
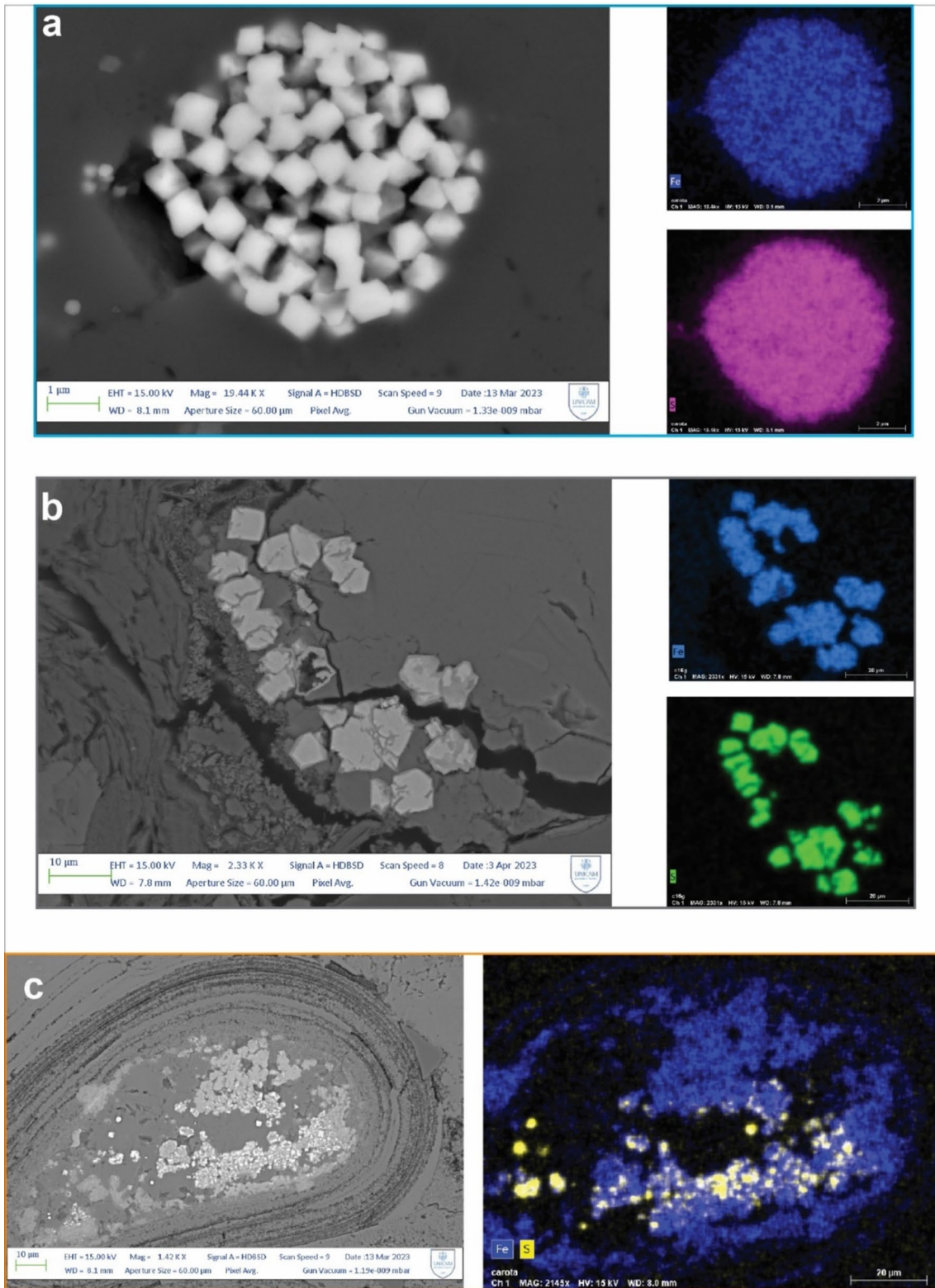
Fig. 16 Different stages of pyrite alteration. For every image, chemical distribution maps were realised: Fe is displayed in blue, and S in pink, green and yellow respectively. **a** Fresh pyrite with no signs of alteration in the core sample from the outcrop. Fe and S are equally distributed and overlapped in the area. **b** First stages of alteration: sulphur oxidation in the grey zone of the column. **c** Advanced stage of alteration: S and Fe oxidation in the ochre zone of the column
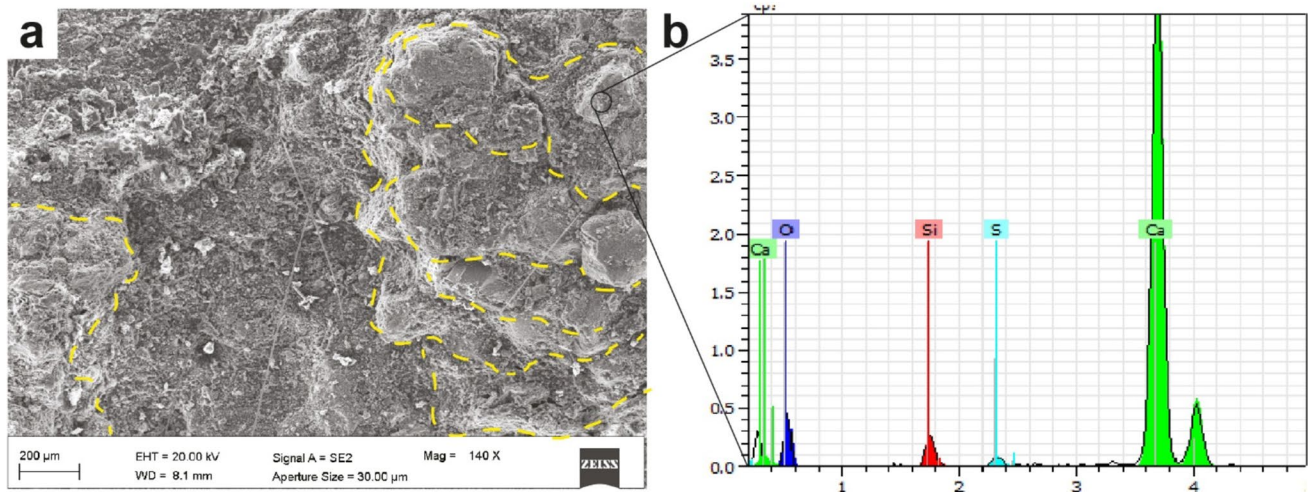
Fig. 17 **a** SEM image acquired in the ochre zone of the column. Outer scales form discontinuity surfaces (highlighted by the dashed yellow lines) which are more compact and richer in Ca. **b** Spectrum with a high calcium peak referred to these case-hardened zones

(diameter < 1 µm), representing the primary porosity of the rock, while only 3–5% of the total pores are macropores. These results suggest that the difference in EQ values between the column samples and the fresh core (mean 472 to 614 L, st. dev. 114 to 81) is mainly due to the development of macroporosity from the expansion and connection of the primary microporosity of the rock, as demonstrated by Liu et al. (2019, 2021). In other words, there is a decrease in micropore volume in favour of an increase in macropore volume in the column, resulting in a similar total open porosity between the column and the fresh core.

Flakes of ochre and grey zones were also analysed to provide mineralogical and petrographic information on the origin of the halos. SEM and RAMAN data have confirmed that the zonation represented by ochre and brown zones has originated from oxyhydroxide–goethite (α-FeOOH), which could develop from the alteration of sulphides and, to a lesser extent, of primary Fe-bearing aluminosilicates (Sebastián et al. 2008; Marszałek et al. 2014). The source of iron for goethite is the pyrite (FeS_2), an accessory mineral in the sandstones of the Camerino Fm., which shows a little alteration in the grey zones (Fig. 16b) in contrast to high oxidation in the ochre colour (Fig. 16c). Goethite has not been detected by XRD in column samples, so its concentration is probably below 3%. However, minimal quantities are sufficient to produce even high pigmentations (Manasse and Mellini 2006).

The alteration represented by the ochre halos is not limited to the column surface but can also be detected in the Orto Botanico outcrop (Fig. 8); the ochre halos can be observed both on the surface of the rock in some places and even close to the rock mass fracture planes, where groundwater circulation takes place. In addition, with advanced weathering, pyrite can be a source of sulphate, which can easily bind to calcium atoms (Xue et al. 2022) to form gypsum ($CaSO_4 \cdot 2H_2O$). Gypsum was detected in trace amounts by the XRD data (Fig. 15) but has been only sporadically detected by SEM since sampling for thin sections was reduced to only a few scales. An acidic environment, coupled with humidity, water vapour and rainwater, favours the dissolution of calcium carbonate and its re-precipitation and reorganisation in the outer and superficial pores (Miandro 1987), forming case-hardened zones in the ochre parts (Fig. 17a). This confirms the higher EQ values with respect to the grey ones, but leads to strong heterogeneities in the alteration of the artefacts and, finally, to the loss of considerable stone material.

Conclusions

This study is aimed at defining a new non-destructive approach for characterising sandstone alteration mechanisms in historically protected buildings, focusing on a portable and easy-to-handle device, named Equotip hardness tester, applicable to soft, porous or easily damaged stone. The advantages of using EQ regard low-impact energy, cost-effectiveness, precise measurement capability and portability and the possibility to involve two different probes for both surface (D probe) and in-depth (DL probe) hardness determination.

The innovative combined use of D and DL probes (for surface and depth measurements), and the regular arrangement of measurements (at predefined heights and orientations), permitted to highlight hardness heterogeneities in the rock surface and in depth.

EQ data in the column surface confirmed the heterogeneous weathering visually assessed by assigning the damage categories of Fitzner et al. (2003). To parity of grain size class, the variability of EQ values in ochre and grey coloured zones has been explained through specific correlations with the porous system and mineralogical composition.

It has been found that grain size can influence hardness data, but above all, there has been a continuous and dense interaction between physical coefficients and high temperature ranges with frost weathering, to which circulation of capillary fluids must be added. Their combined action has expanded and connected many micropores into macropores, explaining the difference in EQ values between column samples and fresh core.

In addition to the physical aspects that have determined a significant increase of the specific surface in the material, de-cohesion can be related to the following chemical processes: (a) pyrite oxidation and release of sulphate ions and iron oxides with the formation of ochre patinas; (b) consequent carbonation of the outer surfaces; (c) pores occlusion which led to case-hardened zones joined with EQ higher values in ochre zones with respect to the grey ones.

This research offers a beneficial contribution to future restoration efforts considering the building's damages following the seismic sequence that struck Central Italy in 2016–2017. The approach needs to be tested on sandstones with different properties and degrees of alteration, in order to highlight the advantages and disadvantages of the methodology. Additionally, it might be a representative example for understanding sandstone decay in historical artworks providing clear quantitative data for decision-makers for their sustainable restoration/conservation.

Declarations

Conflict of interest The authors declare no competing interests.

References

Adamovic J, Mikulas R, Schweigstillova J, Bohmova V (2011) Porosity changes induced by salt weathering of sandstones, Bohemian Cretaceous Basin, Czech Republic. Acta Geodyn Geomater 8:29–46

Aksoy R, İnce İ, Mimiroğlu İM, Esen Ö (2021) Provenance and geological and geomechanical properties of building stones used in the construction of the lyrbe ancient city (Manavgat, Antalya, Turkey). Environ Earth Sci 80:789. https://doi.org/10.1007/s12665-021-10110-0

Al-Naddaf M, Wakid F, Abu Alhassan Y (2012) Micro-drilling resistance measurement: a new technique to estimate the porosity of a building stone. Mediterr Archaeol Archaeom 13:225–233

Alberti AP, Gomes A, Trenhaile A et al (2013) Correlating river terrace remnants using an equotip hardness tester: an example from the Miño River, northwestern Iberian Peninsula. Geomorphology 192:59–70. https://doi.org/10.1016/j.geomorph.2013.03.017

Alexandrowicz Z, Marszałek M, Rzepa G (2014) Distribution of secondary minerals in crusts developed on sandstone exposures: distribution of crusts developed on sandstone exposures. Earth Surf Process Landf 39:320–335. https://doi.org/10.1002/esp.3449

Andreini M, De Falco A, Giresini L, Sassu M (2014) Mechanical characterization of masonry walls with chaotic texture: procedures and results of In-Situ tests. Int J Archit Herit 8:376–407. https://doi.org/10.1080/15583058.2013.826302

Aoki H, Matsukura Y (2007) A new technique for non-destructive field measurement of rock-surface strength: an application of the Equotip hardness tester to weathering studies. Earth Surf Process Landf 32:1759–1769. https://doi.org/10.1002/esp.1492

Aoki H, Matsukura Y (2008) Estimating the unconfined compressive strength of intact rocks from Equotip hardness. Bull Eng Geol Environ 67:23–29. https://doi.org/10.1007/s10064-007-0116-z

Aydin A (2014) ISRM suggested method for determination of the Schmidt hammer rebound hardness: revised version. In: Ulusay R (ed) The ISRM suggested methods for Rock characterization, testing and monitoring: 2007–2014. Springer, pp 25–33

Bai Y, Thompson G, Martinez-Ramirez S, Brueggerhoff S (2003) Mineralogical study of salt crusts formed on historic building stones. Sci Total Environ 302:247–251. https://doi.org/10.1016/S0048-9697(02)00339-X

Basu A, Celestino TB, Bortolucci AA (2009) Evaluation of rock mechanical behaviors under uniaxial compression with reference to assessed weathering grades. Rock Mech Rock Eng 42:73–93. https://doi.org/10.1007/s00603-008-0170-2

Belfiore CM, Barca D, Bonazza A et al (2013) Application of spectrometric analysis to the identification of pollution sources causing cultural heritage damage. Environ Sci Pollut Res 20:8848–8859. https://doi.org/10.1007/s11356-013-1810-y

Benavente D, García del Cura MA, Fort R, Ordóñez S (2004) Durability estimation of porous building stones from pore structure and strength. Eng Geol 74:113–127. https://doi.org/10.1016/j.enggeo.2004.03.005

Bozdağ A, İnce İ, Bozdağ A et al (2020) An assessment of deterioration in cultural heritage: the unique case of Eflatunpınar Hittite Water Monument in Konya, Turkey. Bull Eng Geol Environ 79:1185–1197. https://doi.org/10.1007/s10064-019-01617-9

Calamita F, Centamore E, Chiocchini U et al (1977) Analisi dell'evoluzione tettonico-sedimentaria dei Bacini minori del

Miocene medio-superiore nell'Appennino Umbro-Marchigiano e Laziale-Abruzzese: 4) Primi risultati relativi allo studio geologico del bacino di Camerino (Marche centro-meridionali). Studi Geol Camerti III:87–108. http://193.204.8.201:8080/jspui/handle/1336/142

Cantisani E, Garzonio CA, Ricci M, Vettori S (2013) Relationships between the petrographical, physical and mechanical properties of some Italian sandstones. Int J Rock Mech Min Sci 60:321–332. https://doi.org/10.1016/j.ijrmms.2012.12.042

Çelik SB, Çobanoğlu İ (2019) Comparative investigation of Shore, Schmidt, and Leeb hardness tests in the characterization of rock materials. Environ Earth Sci 78:554. https://doi.org/10.1007/s12665-019-8567-7

Çelik SB, Çobanoğlu İ (2023) Investigation of the effect of saturated conditions and number of measurements on the Leeb hardness test and improved correlations to estimate basic rock properties. Acta Geotech. https://doi.org/10.1007/s11440-023-01823-6

Çelik MY, Sert M (2020) The role of different salt solutions and their concentration ratios in salt crystallization test on the durability of the Döğer tuff (Afyonkarahisar, Turkey) used as building stones of cultural heritages. Bull Eng Geol Environ 79:5553–5568. https://doi.org/10.1007/s10064-020-01896-7

Chen W, Liao R, Wang N, Zhang J (2019) Effects of experimental frost–thaw cycles on sandstones with different weathering degrees: a case from the Bingling Temple grottoes, China. Bull Eng Geol Environ 78:5311–5326. https://doi.org/10.1007/s10064-018-01454-2

Christaras B, Moropoulou A, Chatziangelou M et al (2016) Comparative surface damage determination at a jewish grave using two different mobile ultrasonic velocity devices. In: Aggelis DG (ed) Emerging technologies in non-destructive testing VI. Taylor & Francis Group, London, pp 383–388

Coombes MA, Feal-Pérez A, Naylor LA, Wilhelm K (2013) A non-destructive tool for detecting changes in the hardness of engineering materials: application of the Equotip durometer in the coastal zone. Eng Geol 167:14–19. https://doi.org/10.1016/j.enggeo.2013.10.003

Cutler NA, Viles HA, Ahmad S et al (2013) Algal 'greening' and the conservation of stone heritage structures. Sci Total Environ 442:152–164. https://doi.org/10.1016/j.scitotenv.2012.10.050

Desarnaud J, Kiriyama K, Simsir BB et al (2019) A laboratory study of Equotip surface hardness measurements on a range of sandstones: what influences the values and what do they mean? EARTH Surf Process Landf 44:1419–1429. https://doi.org/10.1002/esp.4584

Fahy MP, Guccione MJ (1979) Estimating strength of sandstone using petrographic thin-section data. Bull Assoc Eng Geol 16:467–485

Feal-Pérez A, Blanco-Chao R (2013) Characterization of abrasion surfaces in rock shore environments of NW Spain. Geo-Mar Lett 33:173–181. https://doi.org/10.1007/s00367-012-0300-4

Fisher RA (1970) Statistical methods for research workers. Breakthroughs in statistics: methodology and distribution. Springer, pp 66–70

Fitzner B, Heinrichs K (2002) Damage diagnosis on stone monuments – weathering forms, damage categories and damage indices. R. Prikryl, H.A. Viles, Karolinum Press, Prague, pp 11–56

Fitzner B, Heinrichs K, Bouchardiere DL (2003) Weathering damage on pharaonic sandstone monuments in Luxor-Egypt. Build Environ 38:1089–1103. https://doi.org/10.1016/S0360-1323(03)00086-6

Fitzner B, Heinrichs K, Kownatzki R (1995) Weathering forms, classification and mapping: Verwitterungsformen-Klassifizierung und Kartierung. Ernst and Sohn, Berlin

Folk RL (1974) Petrology of sedimentary rocks: Austin. Tex Hemphill 182

Fort R, Alvarez de Buergo M, Perez-Monserrat EM (2013) Non-destructive testing for the assessment of granite decay in heritage structures compared to quarry stone. Int J Rock Mech Min Sci 61:296–305. https://doi.org/10.1016/j.ijrmms.2012.12.048

Frattali A (1999) Caratteri mineralogico-petrografici, fenomeni di alterazione e provenienza delle arenarie dei monumenti di Camerino. Tesi Sperimentale di Laurea in Mineralogia, Università degli Studi di Camerino

Götze J, Siedel H (2004) Microscopic scale characterization of ancient building sandstones from Saxony (Germany). Mater Charact 53:209–222. https://doi.org/10.1016/j.matchar.2004.08.016

Goudie AS (2006) The Schmidt Hammer in geomorphological research. Prog Phys Geogr Earth Environ 30:703–718. https://doi.org/10.1177/0309133306071954

Hatır ME, Korkanç M, Başar ME (2019) Evaluating the deterioration effects of building stones using NDT: the Küçükköy Church, Cappadocia Region, central Turkey. Bull Eng Geol Environ 78:3465–3478. https://doi.org/10.1007/s10064-018-1339-x

Huang S, Yu S, Ye Y et al (2022) Pore structure change and physico-mechanical properties deterioration of sandstone suffering freeze-thaw actions. Constr Build Mater 330:127200. https://doi.org/10.1016/j.conbuildmat.2022.127200

İnce İ, Bozdağ A, Tosunlar MB et al (2018) Determination of deterioration of the main facade of the Ferit Paşa Cistern by non-destructive techniques (Konya, Turkey). Environ Earth Sci 77:420. https://doi.org/10.1007/s12665-018-7595-z

Jeannette D (1997) Importance of the pore structures during the weathering process of stones in monuments. Soils and sediments. Springer Berlin Heidelberg, Berlin, Heidelberg, pp 177–190

Jia H, Ding S, Wang Y et al (2019) An NMR-based investigation of pore water freezing process in sandstone. Cold Reg Sci Technol 168:102893. https://doi.org/10.1016/j.coldregions.2019.102893

Jiménez-González I, Rodríguez-Navarro C, Scherer GW (2008) Role of clay minerals in the physicomechanical deterioration of sandstone. J Geophys Res Earth Surf 113

Kawasaki S, Tanimoto C, Koizumi K, Ishikawa M (2002) An attempt to estimate mechanical properties of rocks using the Equotip hardness tester. J Jpn Soc Eng Geol 43:244–248

Kompatscher M (2004) Equotip-rebound hardness testing after D. Leeb. In: Proceedings, conference on hardness measurements theory and application in laboratories and industries. pp 1–12

Kong F, Xue Y, Qiu D et al (2021) Effect of grain size or anisotropy on the correlation between uniaxial compressive strength and Schmidt hammer test for building stones. Constr Build Mater 299:123941. https://doi.org/10.1016/j.conbuildmat.2021.123941

Korkanç M, İnce İ, Hatır ME, Tosunlar MB (2021) Atmospheric and anthropogenic deterioration of the İvriz rock monument: Ereğli-Konya, Central Anatolia, Turkey. Bull Eng Geol Environ 80:3053–3063. https://doi.org/10.1007/s10064-021-02105-9

Kósa Z, Török Á (2020) Characterization of historic binders and stones of a ruined medieval church (Hungary). https://doi.org/10.3311/PPci.15599. Period Polytech Civ Eng

Labus M, Bochen J (2012) Sandstone degradation: an experimental study of accelerated weathering. Environ Earth Sci 67:2027–2042. https://doi.org/10.1007/s12665-012-1642-y

Le T-T, Skentou AD, Mamou A, Asteris PG (2022) Correlating the unconfined compressive strength of rock with the compressional wave velocity effective porosity and Schmidt Hammer rebound number using artificial neural networks. Rock Mech Rock Eng 55:6805–6840. https://doi.org/10.1007/s00603-022-02992-8

Leeb D (1979) Dynamic hardness testing of metallic materials. NDT Int 12:274–278

Liu B, Ma Y, Liu N et al (2019) Investigation of pore structure changes in mesozoic water-rich sandstone induced by freeze-thaw process under different confining pressures using digital rock technology.

Cold Reg Sci Technol 161:137–149. https://doi.org/10.1016/j.coldregions.2019.03.006

Liu T, Zhang C, Li J et al (2021) Detecting freeze–thaw damage degradation of sandstone with initial damage using NMR technology. Bull Eng Geol Environ 80:4529–4545. https://doi.org/10.1007/s10064-021-02242-1

Lombillo I, Thomas C, Villegas L et al (2013) Mechanical characterization of rubble stone masonry walls using non and minor destructive tests. Constr Build Mater 43:266–277. https://doi.org/10.1016/j.conbuildmat.2013.02.007

Ludovico-Marques M, Chastre C, Vasconcelos G (2012) Modelling the compressive mechanical behaviour of granite and sandstone historical building stones. Constr Build Mater 28:372–381. https://doi.org/10.1016/j.conbuildmat.2011.08.083

Mammoliti E, Ferretti A, Malavolta M et al (2021) Defining a non-destructive in situ approach for the determination of historical mortar strength using the Equotip hardness tester. Appl Sci 11:4788. https://doi.org/10.3390/app11114788

Mammoliti E, Teloni R, Cupido M, Malavolta M (2023) Studio sedimentologico e geomeccanico delle arenarie delle colonne del porticato di Palazzo Ducale e dell'affioramento dell'Orto Botanico - Relazione tecnico-illustrativa (Technical report)

Manasse A, Mellini M (2006) Iron (hydr)oxide nanocrystals in raw and burnt sienna pigments. Eur J Mineral 18:845–853. https://doi.org/10.1127/0935-1221/2006/0018-0845

Manganelli Del, Fà R, Riminesi C, Rescic S et al (2016) NDT to perform service of the evaluation of conservation works. In: Aggelis DG (ed) Emerging technologies in non-destructive testing VI. Taylor & Francis Group, London, pp 457–463

Marszałek M, Alexandrowicz Z, Rzepa G (2014) Composition of weathering crusts on sandstones from natural outcrops and architectonic elements in an urban environment. Environ Sci Pollut Res 21:14023–14036. https://doi.org/10.1007/s11356-014-3312-y

Mattias P, Capaccioni B, Vaselli O (1996) L'arenaria Di Palazzo Ducale in Camerino (MC): Caratteristiche mineralogico-petrografiche e considerazioni sullo stato di conservazione. Studi Geol Camerti XIV:67–82

McGreevy JP (1985) A preliminary scanning electron microscope study of honeycomb weathering of sandstone in a coastal environment. Earth Surf Process Landf 10:509–518. https://doi.org/10.1002/esp.3290100509

Meng Z, Zhang J, Peng S (2006) Influence of sedimentary environments on mechanical properties of clastic rocks. Environ Geol 51:113–120. https://doi.org/10.1007/s00254-006-0309-y

Miandro R (1987) Gli aspetti mineralogico-petrografici Del processo di alterazione dell'arenaria del Palazzo Ducale Di Camerino: 2) Degrado delle strutture interne del palazzo. Tesi Sperimentale di Laurea in Mineralogia, Università degli Studi di Camerino

MIC - Ministero della Cultura (2023) Siti italiani del Patrimonio Mondiale UNESCO. In: Minist. Beni E Attiv. Cult. E Il Tur. https://www.beniculturali.it/sitiunesco. Accessed 8 Mar 2023

Mohamad ET, Komoo I, Kassim KA, Gofar N (2008) Influence of moisture content on the strength of weathered sandstone. Malays J Civ Eng 20:137–144

Mol L, Viles HA (2012) The role of rock surface hardness and internal moisture in tafoni development in sandstone. Earth Surf Process Landf 37:301–314. https://doi.org/10.1002/esp.2252

Molina E, Cultrone G, Sebastián E et al (2011) The pore system of sedimentary rocks as a key factor in the durability of building materials. Eng Geol 118:110–121. https://doi.org/10.1016/j.enggeo.2011.01.008

Olmi R, Riminesi C, Rosina E (2016) Integration of EFD, MRM and IRT for moisture mapping on historic masonry: study cases in northern Italy. Emerging technologies in non-destructive testing VI. Taylor & Francis Group, London, pp 471–476

Pamplona M, Kocher M, Snethlage R, Barros LA (2007) Drilling resistance: overview and outlook. Z Dt Ges Geowiss 158/3:665–676. https://doi.org/10.1127/1860-1804/2007/0158-0665

Pappalardo G, Mineo S, Caliò D, Bognandi A (2022) Evaluation of natural stone weathering in heritage building by infrared thermography. Heritage 5:2594–2614. https://doi.org/10.3390/heritage5030135

Paraventi M (2003) I da Varano e le arti a Camerino e nel territorio: atlante dei beni culturali di epoca varanesca. Bieffe

Popovics JS (2003) NDE techniques for concrete and masonry structures. Prog Struct Eng Mater 5:49–59. https://doi.org/10.1002/pse.146

Přikryl R, Snížek P (2023) Critical assessment of the non-destructiveness of Schmidt hammer test on monumental sandstones: a microscopic and microstructural approach. J Cult Herit 59:247–254. https://doi.org/10.1016/j.culher.2022.12.011

Přikryl R, Weishauptová Z, Novotná M et al (2011) Physical and mechanical properties of the repaired sandstone ashlars in the facing masonry of the Charles Bridge in Prague (Czech Republic) and an analytical study for the causes of its rapid decay. Environ Earth Sci 63:1623–1639

Proceq© SA (2010) Operating instructions portable metal hardness tester. https://www.screeningeagle.com/en/products/category/metal/equotip. Accessed 12 May 2023

Qi Y, Ju Y, Yu K et al (2022) The effect of grain size, porosity and mineralogy on the compressive strength of tight sandstones: a case study from the eastern Ordos Basin, China. J Pet Sci Eng 208:109461. https://doi.org/10.1016/j.petrol.2021.109461

Roduit N (2019) JMicroVision: Image analysis toolbox for measuring and quantifying components of high-definition images

Salvatici T, Calandra S, Centauro I et al (2020) Monitoring and evaluation of sandstone decay adopting non-destructive techniques: on-site application on building stones. Heritage 3:1287–1301. https://doi.org/10.3390/heritage3040071

Schuller MP (2003) Nondestructive testing and damage assessment of masonry structures. Prog Struct Eng Mater 5:239–251. https://doi.org/10.1002/pse.160

Sebastián E, Cultrone G, Benavente D et al (2008) Swelling damage in clay-rich sandstones used in the church of San Mateo in Tarifa (Spain). J Cult Herit 9:66–76. https://doi.org/10.1016/j.culher.2007.09.002

Shakoor A, Bonelli RE (1991) Relationship between petrographic characteristics, engineering index properties, and mechanical properties of selected sandstones. Bull Assoc Eng Geol 28:55–71

Siedel H, Pfefferkorn S, von Plehwe-Leisen E, Leisen H (2010) Sandstone weathering in tropical climate: results of low-destructive investigations at the temple of Angkor Wat, Cambodia. Eng Geol 115:182–192. https://doi.org/10.1016/j.enggeo.2009.07.003

Siegesmund S, Weiss T, Vollbrecht A (2002) Natural stone, weathering phenomena, conservation strategies and case studies: introduction. Geol Soc Lond Spec Publ 205:1–7. https://doi.org/10.1144/GSL.SP.2002.205.01.01

Singh SK (1988) Relationship among fatigue strength, mean grain size and compressive strength of a rock. Rock Mech Rock Eng 21:271–276

Soroush H (2008) A rapid method for real-time evaluation of formation strength. In: The 42nd US Rock Mechanics Symposium (USRMS). OnePetro

Sumner P, Nel W (2002) The effect of rock moisture on Schmidt hammer rebound: tests on rock samples from Marion Island and South Africa. Earth Surf Process Landf 27:1137–1142. https://doi.org/10.1002/esp.402

Theodoridou M, Török Á (2019) In situ investigation of stone heritage sites for conservation purposes: a case study of the Székesfehérvár Ruin Garden in Hungary. Prog Earth Planet Sci 6:15. https://doi.org/10.1186/s40645-019-0268-z

Tonon C, Bernasconi D, Martire L et al (2022) Lichen impact on sandstone hardness is species-specific. Earth Surf Process Landf 47:1147–1156. https://doi.org/10.1002/esp.5307

Török Á (2003) Surface strength and mineralogy of weathering crusts on limestone buildings in Budapest. Build Environ 38:1185–1192

Török Á (2008) Black crusts on travertine: factors controlling development and stability. Environ Geol 56:583–594

Török Á, Forgó LZ, Vogt T et al (2007) The influence of lithology and pore-size distribution on the durability of acid volcanic tuffs, Hungary. Geol Soc Lond Spec Publ 271:251–260. https://doi.org/10.1144/GSL.SP.2007.271.01.24

Török Á, Přikryl R (2010) Current methods and future trends in testing, durability analyses and provenance studies of natural stones used in historical monuments. Eng Geol 115:139–142. https://doi.org/10.1016/j.enggeo.2010.07.003

Turkington AV, Paradise TR (2005) Sandstone weathering: a century of research and innovation. Geomorphology 67:229–253. https://doi.org/10.1016/j.geomorph.2004.09.028

Vasanelli E, Sileo M, Calia A, Aiello MA (2013) Non-destructive techniques to assess mechanical and physical properties of Soft Calcarenitic stones. Procedia Chem 8:35–44. https://doi.org/10.1016/j.proche.2013.03.006

Veniale F, Setti M, Rodríguez-Navarro C, Lodola S (2001) Procesos de alteración asociados al contenido de minerales arcillosos en materiales pétreos. Mater Constr 51:163–182. https://doi.org/10.3989/mc.2001.v51.i263-264.362

Vergès-Belmin V (2008) Illustrated glossary on stone deterioration patterns. ICOMOS International Scientific Committee for Stone (ISCS)Icomos

Verstrynge E, Adriaens R, Elsen J, Van Balen K (2014) Multi-scale analysis on the influence of moisture on the mechanical behavior of ferruginous sandstone. Constr Build Mater 54:78–90. https://doi.org/10.1016/j.conbuildmat.2013.12.024

Viles H, Camuffo D, Fitz S, Baer NS, Snethlage R et al (1997) Chichester, Wiley, 95–112

Viles H, Goudie A, Grab S, Lalley J (2011) The use of the Schmidt Hammer and Equotip for rock hardness assessment in geomorphology and heritage science: a comparative analysis. Earth Surf Process Landf 36:320–333. https://doi.org/10.1002/esp.2040

Wang Y, Zhang H (2023) The synergic impacts of salt mixture and frost damage on rock decay: implications for the deterioration of rock-hewn heritages. Herit Sci 11:209. https://doi.org/10.1186/s40494-023-01054-8

Wang Y, Pei Q, Yang S et al (2020) Evaluating the condition of Sandstone Rock-Hewn Cave-Temple Façade using in situ non-invasive techniques. Rock Mech Rock Eng 53:2915–2920. https://doi.org/10.1007/s00603-020-02063-w

Wang Y, Shao M, Zhang J et al (2021) Quantitative evaluation of alteration and exfoliation in jurassic sandstone, Chongqing Danzishi rock carvings, China. Eng Geol 292:106277. https://doi.org/10.1016/j.enggeo.2021.106277

Wilhelm K, Viles H, Burke Ó (2016) Low impact surface hardness testing (Equotip) on porous surfaces - advances in methodology with implications for rock weathering and stone deterioration research: Equotip hardness testing on porous rock and stone. Earth Surf Process Landf 41:1027–1038. https://doi.org/10.1002/esp.3882

Williams RBG, Robinson DA (1983) The effect of surface texture on the determination of the surface hardness of rock using the schmidt hammer. Earth Surf Process Landf 8:289–292. https://doi.org/10.1002/esp.3290080311

Witzany J, Cejka T, Zigler R (2010) The effect of moisture on significant mechanical characteristics of masonry. Eng Struct Technol 2:79–85. https://doi.org/10.3846/skt.2010.11

Xue J, Fuchida S, Ishida S, Tokoro C (2022) Insight on exogenous calcium/magnesium in weakening pyrite floatability with prolonged pre-oxidation: localized and concomitant secondary minerals and their depression characteristics. Minerals 12:115. https://doi.org/10.3390/min12020115

Yılmaz NG (2013) The influence of testing procedures on uniaxial compressive strength prediction of carbonate rocks from Equotip hardness tester (EHT) and proposal of a new testing methodology: hybrid dynamic hardness (HDH). Rock Mech Rock Eng 46:95–106. https://doi.org/10.1007/s00603-012-0261-y

Zhang J, Huang J, Liu J et al (2019) Surface weathering characteristics and degree of Niche of Sakyamuni entering Nirvana at Dazu Rock Carvings, China. Bull Eng Geol Environ 78:3891–3899. https://doi.org/10.1007/s10064-018-1424-1